OPEN FILE REPORT OFR 06-01

Arizona Geological Survey
416 W. Congress St. #100 Tucson, Az
www.azgs.az.gov

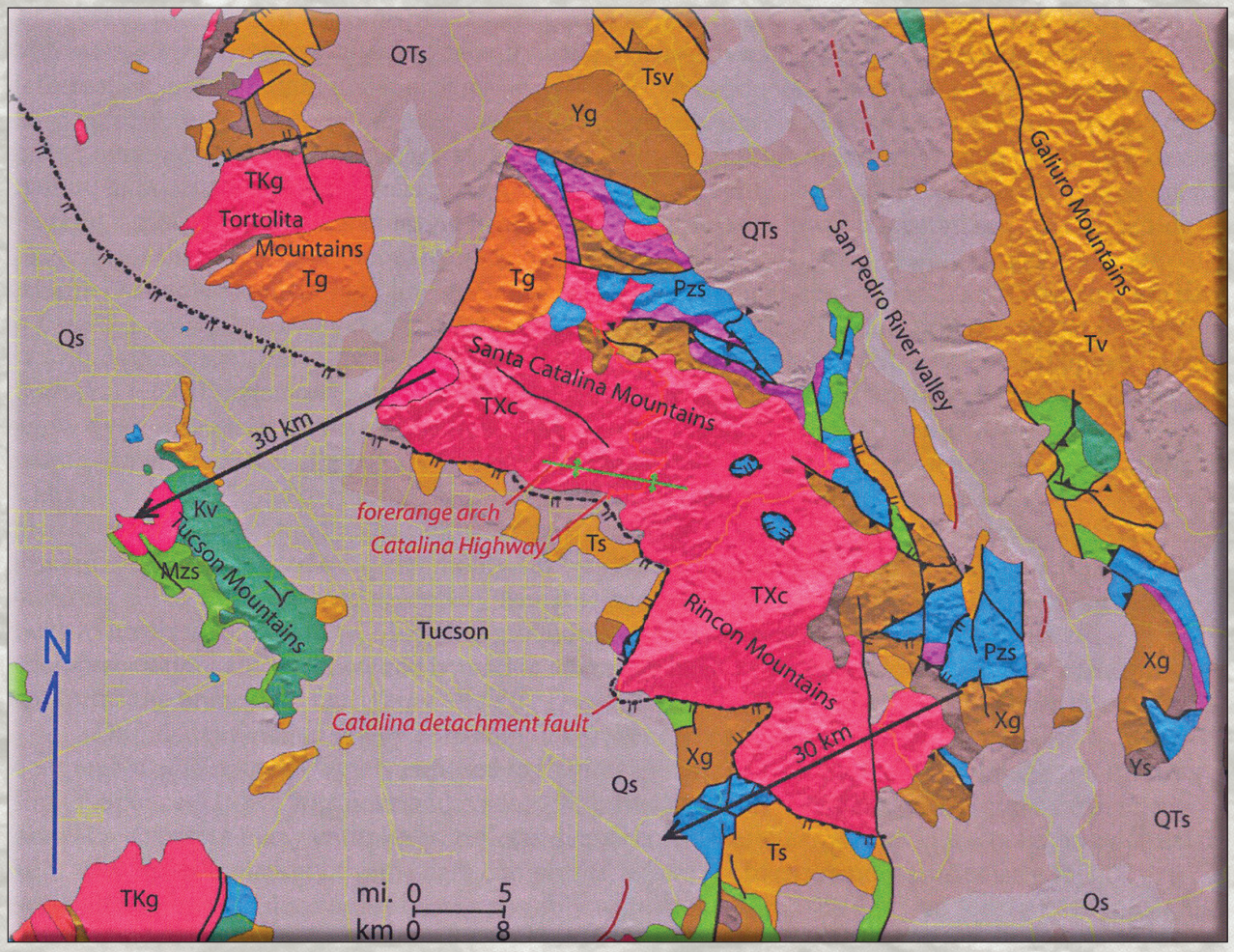

A Geologist's Guide to the Core Complex Geology Along the Catalina Highway, Tucson Area, Arizona

version 1.1
June, 2006

JON E. SPENCER
ARIZONA GEOLOGICAL SURVEY

A geologist's guide to the core complex geology along the Catalina Highway, Tucson area, Arizona

Jon. E. Spencer
Arizona Geological Survey
416 W. Congress St., Suite 100, Tucson, AZ 85701

Arizona Geological Survey Open File Report 06-01
version 1.1

June, 2006

38 p. text

www.azgs.az.gov

A geologist's guide to the core complex geology along the Catalina Highway, Tucson area, Arizona

Jon E. Spencer
Arizona Geological Survey

TABLE OF CONTENTS

INTRODUCTION

The Catalina Highway, which extends from the Tucson metropolitan area up the south side of the Santa Catalina Mountains to the top of the range, provides easy access to some very interesting geology as well as spectacular views and an escape from the summer heat. The south flank of the range, if not the entire range, was uplifted and uncovered from deep beneath the Tucson basin and Tucson Mountains by several tens of kilometers of top-SW displacement on the Catalina detachment fault*, an Oligo-Miocene low-angle normal fault (e.g., Dickinson, 1991). This fault dips gently southward beneath the Tucson Basin and is exposed at only a few small localities on private property at the foot of the range. This shallowly buried fault is better exposed to the southeast where it follows a sinuous course at the foot of the Rincon Mountains (Fig. 1). The northern part of the Tucson basin is largely a half graben in the hanging wall of this fault.

All of the rocks visible along the highway make up the footwall block of the Catalina detachment fault. These rocks consist dominantly of Eocene muscovite leucogranite and pegmatite sills within Proterozoic granite, with middle Proterozoic and Paleozoic metasedimentary rocks preserved at the crest of the range (Keith et al., 1980; Force, 1997). The foliated leucogranites and banded gneisses visible along the highway were emplaced and deformed in the middle crust, at depths of perhaps 8 to 15 km, until Oligo-Miocene tectonic exhumation uplifted and uncovered them and tilted the range to the northeast. Shearing in the middle crust, down dip from the detachment fault during its early movement history, produced mylonitic fabrics in these rocks that are the primary focus of this field guide. Asymmetric petrofabrics that allow determination of shear sense in the mylonitic rocks reveal a complex history of deformation. This field guide is directed primarily at observing these mylonitic fabrics and evaluating their shear-sense indicators, and is also a guide to some short hikes to scenic areas with interesting core-complex geology.

*A detachment fault is a gently to moderately dipping, low-angle normal fault with large displacement (usually tens of kilometers)

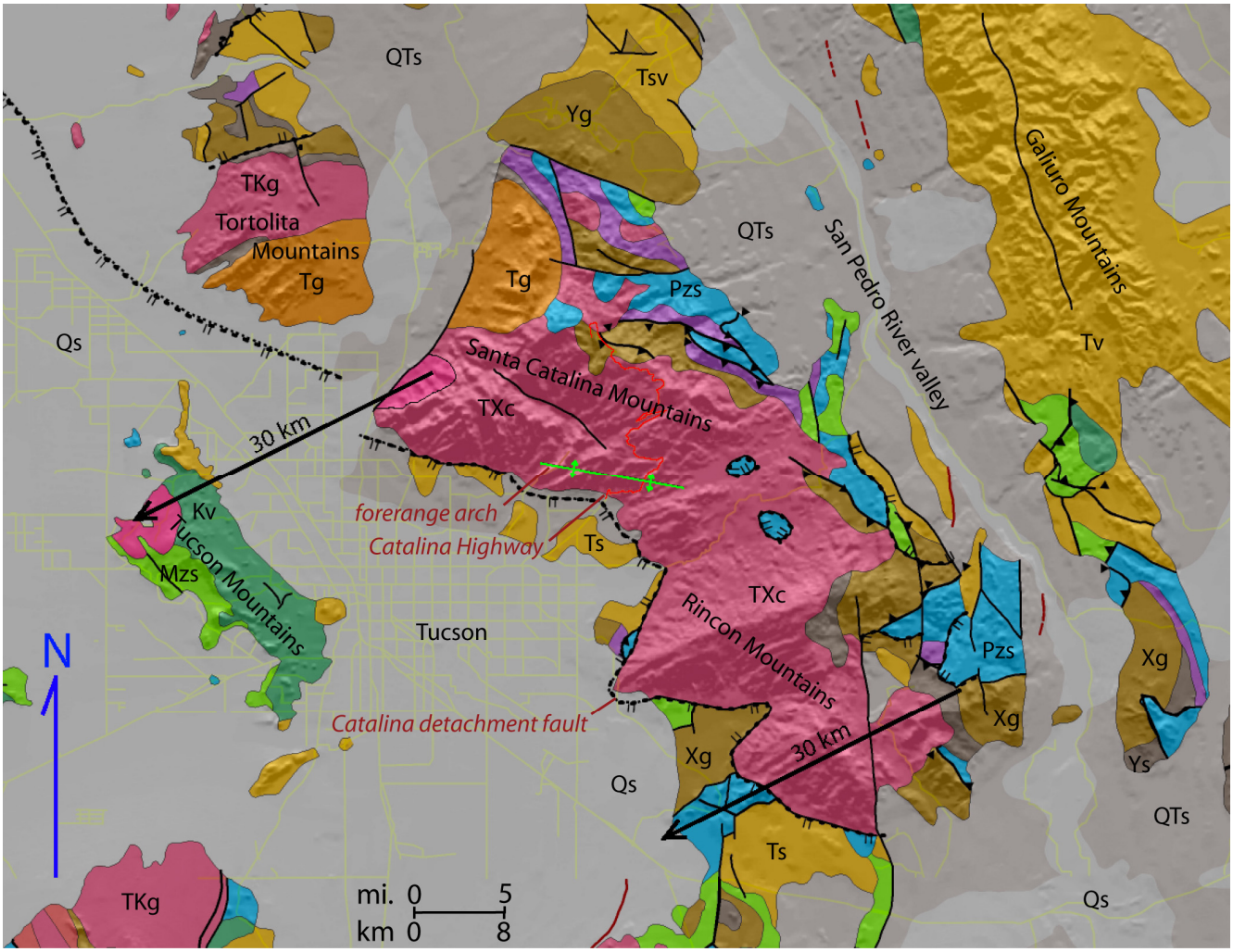

Figure 1. Geologic map of the Santa Catalina and Rincon Mountains and nearby ranges. The southwest side of the Tortolita Mountains are mylonitic and this range is part of the Catalina metamorphic core complex. The two 30 km vectors represent estimated offset of the Catalina detachment fault.

What is a metamorphic core complex?

Most active faults within continents project down dip across the brittle-ductile transition and into the middle crust where temperatures are above about 300° C, quartz deforms plastically, and seismicity and brittle faulting are reduced or absent. Mylonitic fabrics are produced in the middle crust where strain is accommodated partly by plastic deformation of some minerals, especially quartz and mica. Such mylonitic rocks cool and become brittle where they are uplifted in the footwalls of normal faults and, if displacement is sufficient, they will be completely exhumed. Areas of exposed mylonitic rocks that were exhumed by large displacement on gently to moderately dipping normal faults are called “metamorphic core complexes” or just “core complexes.” In many metamorphic core complexes, such as the Catalina core complex, mylonitic rocks were exhumed and eroded to produce mylonitic debris that was shed into hanging-wall basins where syn-tectonic conglomerates were faulted and tilted during continued normal faulting. Such conglomerates, exposed in the Catalina foothills, are a good example of the consequences of geologically rapid tectonic exhumation whereby mid-crustal granites and gneisses were mylonitized and became conglomerate debris during the course of just a few million years.

The footwalls of large-displacement, gently to moderately dipping normal faults associated with metamorphic core complexes generally have a distinctive suite of rock types that reflect deformation and alteration under progressively lower temperatures. Indeed, this is perhaps the defining feature of metamorphic core complexes. Variably developed mylonitic fabrics exposed over tens to hundreds of meters of structural thickness below a large-displacement normal fault may be cut by thin, high-strain mylonitic shear zones. Such late-developing shear zones are more common near the fault surface and reflect increasing localization of strain with lower temperatures. In this setting quartz veins that are subparallel to shear zones appear to have localized shearing so that some are extremely strained and strongly lineated. During tectonic exhumation, footwall rocks became too cool to deform plastically as they passed upward through the brittle-ductile transition and began deforming by brittle processes. Early-formed fractures are generally somewhat distributed, occurring over several to several tens of meters below the fault. Rocks that were fractured and brecciated at temperatures just below those necessary for mylonitization (~300° C) are typically greenish because of alteration by hydrothermal fluids traveling along fractures. Rocks strongly affected by such alteration are known as "chloritic breccia." In extreme cases, severe chloritic alteration of strongly brecciated to microbrecciated crystalline rocks produced dark green rocks in which protolith compositions are obscure. Chloritic breccias are commonly cut by younger, hematite-coated fractures. Influx of oxidizing fluids that produced secondary hematite occurred when tectonic exhumation brought these rocks to levels where shallow, oxidizing groundwater gained access to the fractured rocks. Microbrecciation, silicification and hematitic alteration have locally produced a smooth, resistant ledge that forms the immediate fault footwall (e.g., Davis, 1980; Davis and Lister, 1988; Smith et al., 1991).

During exhumation, many core complexes were flexed and tilted to form arched or domed topographic edifices with widely exposed mylonitic and gneissic rocks derived from the middle crust (Fig. 2; Spencer, 1984; Wernicke and Axen, 1988; Buck, 1988). The corrugated form of exhumed footwalls, apparent many complexes, reflects displacement-parallel grooves in the bounding normal fault. During exhumation of some core complexes, where grooves are now particularly long, plastically deforming deep crustal rocks possibly were molded into the grooved form of the colder and stronger underside of the hanging wall (Spencer, 1999). Tanque Verde Ridge, which makes up the northern Rincon Mountains and is clearly visible to the southeast from the Catalina Highway, is one of the largest known antiformal corrugations in a metamorphic core complex.

Arizona's metamorphic core complexes were uncovered in the late Oligocene and early to middle Miocene (roughly 30 to 12 Ma) and have not been severely degraded by erosion since footwall exhumation. Typically, chloritic breccias and other fractured footwall rocks have been eroded away, but underlying crystalline rocks are sufficiently well preserved that it is possible to discern the original form of the arched normal faults that once extended over the complexes (Pain, 1985). These faults were grooved on a scale of many kilometers so that long ridges such as Tanque Verde Ridge in the Rincon Mountains, the South Mountains south of Phoenix, and the Harcuvar Mountains in western Arizona are enormous, erosionally degraded fault grooves (Spencer, 2000).

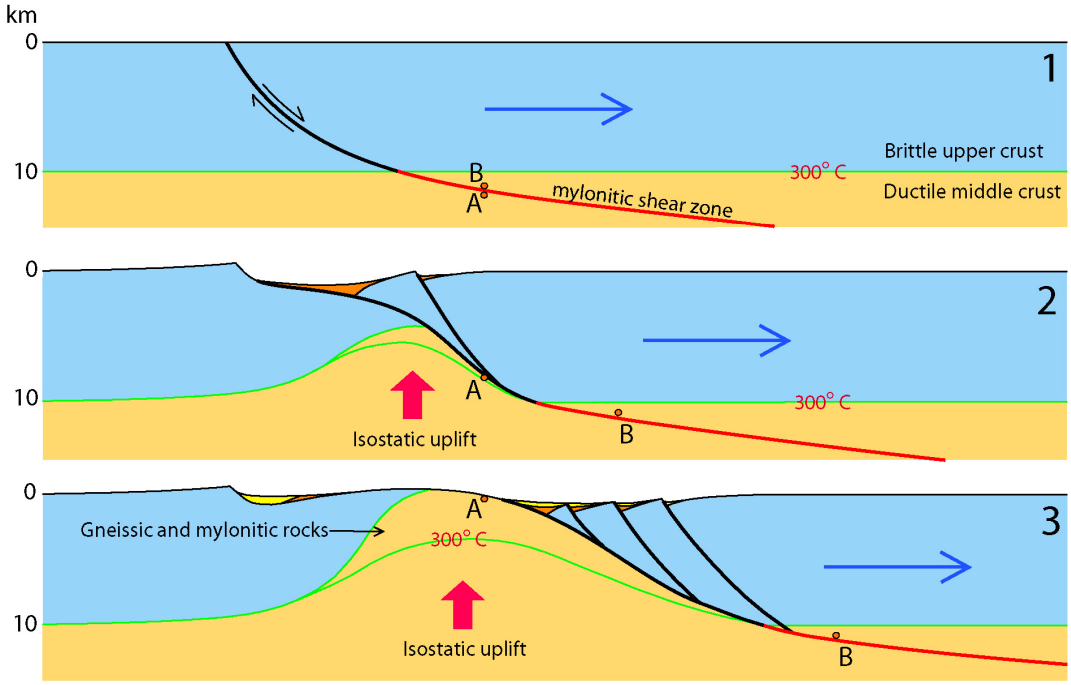

Figure 2. Idealized cross sectional evolution of extensional exhumation of a metamorphic core complex. Rocks at point A are uplifted isostatically in response to tectonic denudation, and travel from the plastically deforming middle crust to the Earth's surface is a few million years. Inflow of hot and mobile middle crust is promoted by syn-magmatic high temperatures and by thick crust with a wide channel for deep crustal flow (Wernicke, 1990, 1992; Kruse et al., 1991).

Sense of shear in mylonites

The well-lineated mylonitic fabrics that are characteristic of metamorphic core complexes were originally linked to extension and tectonic exhumation because lineation is generally parallel to extension direction in nearby faulted hanging-wall rocks (e.g., Davis, 1980). Identification of mylonitic shear-sense indicators in many core complexes has confirmed this inference by showing that the mylonitic shear zones accommodated normal-sense shear (e.g., Davis et al., 1986; Naruk, 1987; Naruk and Bykerk-Kauffman, 1990; Reynolds and Lister, 1990). This supports the view that mylonitic fabrics originated during extensional exhumation and are not older fabrics unrelated to mid-Cenozoic extension (e.g., Drewes, 1977).

Three types of structures have been very useful in determining shear sense in the field in Arizona core-complex mylonites. These features, known as asymmetric mylonitic petrofabrics, are identified on rock surfaces that are approximately parallel to mylonitic lineation and perpendicular to foliation. These features are as follows: (1) S-C mylonites contain two fabric elements, one a planar fabric that originated largely or entirely by flattening, with mineral growth, especially in mica, perpendicular to the flattening vector (the S surface, "S" for schistosity), and the other represented by somewhat to highly discreet or localized shear zones (the C surface, "C" for *cisaillement*, or shear) that are slightly to moderately discordant to the flattening fabric. Typically, the planar schistosity appears to have been dragged into parallelism with the shear zones at the shear-zone margins (Fig. 3). S-C mylonites are thought to develop during a single period of flattening and shearing, but with heterogeneous development of simple-shear strain and perhaps some diachroneity between flattening and simple shear (Berthé et al., 1979; Lister and Snoke, 1984). (2) Asymmetric tails on porphyroclasts represent zones where, typically, K-feldspar is broken into small fragments at porphyroclast margins and displaced by shearing into the surrounding, finer grained matrix (Fig. 4). The asymmetric

disposition of the crushed tails about the porphyroclast reveal the sense of shear (e.g., Simpson and Schmid, 1983). Asymmetric tails on mica grains, visible in thin section, provide shear sense in the same manner (e.g., Lister and Snoke, 1984). (3) Some porphyroclasts with asymmetric tails are rolled during shearing. The sheared-out tails, near the rolled porphyroclast, are rolled with the porphyroclast, whereas farther from the porphyroclast the tails are not rolled (Figs. 5, 6, 7). Shear sense is apparent from the sense of rolling (e.g., Mawer, 1987; Hanmer and Passchier, 1991).

In addition to these criteria, statistically preferred orientations of quartz c-axes may also reveal sense of shear when viewed with a petrographic microscope. Quartz veins in core-complex mylonites, especially if oriented subparallel to mylonitic foliation, commonly underwent severe grain-size reduction just before cooling through the brittle-ductile transition (Fig. 9A). In thin sections cut parallel to mylonitic lineation and perpendicular to foliation, hundreds of quartz subgrains form elongate clusters or bands with similar but not identical crystallographic orientation of each subgrain, and each quartz subgrain is commonly elongate and tilted forward in the direction of shear (Figs. 9B, E). Many studies of quartz c-axis orientations in such quartz-bearing mylonitic rocks have revealed a characteristic statistical preferred orientation, with most c-axes at a high angle to lineation but tilted slightly in a manner that is consistent with quartz-subgrain elongation and with shear sense as determined by other criteria (Fig. 8; e.g., Lister and Snoke, 1984). This slight forward tilting can be discerned in thin section by inserting the quartz plate into the petrographic microscope and rotating the stage. Dominantly blue colors appear when the optically slow and fast directions in the quartz subgrains are statistically aligned with the slow and fast directions, respectively, in the quartz plate (optically additive), and dominantly yellow and orange colors appear when the slow and fast directions are statistically aligned with the fast and slow directions, respectively, of the quartz plate (optically subtractive). By rotating the stage one can determine the statistically dominant c-axis direction to within a few degrees for both the additive and subtractive configurations (Fig. 9). These will be ~90° apart if c-axis orientations are statistically highly parallel. If they are highly parallel, discordance between the dominant c-axis orientation and the perpendicular to the shear plane (as determined by streaked out mica grains or other mineral aggregates) may reveal the sense of shear (Fig. 9H).

The Catalina core complex in the history of core-complex studies

By the 1970s a long history of studies of gneissic and high grade metamorphic rocks in orogenic belts had generally determined that such rocks were displaced from great depths by thrust faulting and folding. As a result of this perspective, identification of metamorphic core complexes as features where gneissic and high-grade metamorphic rocks were exhumed during severe extension required many field investigations to document a recurring and previously undocumented set of geologic features, and some conceptual breakthroughs. The term “metamorphic core complex” was coined by UA Professor Peter Coney to apply to metamorphic complexes in the core of the Cordilleran orogen. Peter was a convener of a Geological Society of America Penrose Conference on Cordilleran metamorphic core complexes, held in 1977 in Tucson, at which the term “metamorphic core complex” entered the geologist’s lexicon, albeit with much controversy surrounding associated interpretations (Crittenden et al., 1980). By the mid 1980s, the geologic community was converging on a consensus that core complexes originated by tectonic exhumation. Shear-sense determinations from mylonitic rocks, including those in the Tucson area, played a significant role in bringing about this consensus view. Since then, core complexes have been identified in many parts of Europe and Asia, the southwestern Pacific rim, in the Andes, in the deep ocean where they are associated with slow-spreading plate divergence, and probably on Venus. The Santa Catalina Mountains have thus played an important role in the recognition of what have turned out to be widespread tectonic features. In addition, their excellent and accessible exposures makes this range ideal for a field introduction to some of the footwall features of metamorphic core complexes.

References cited

Berthé, D., Choukroune, P., and Jegouzo, P., 1979, Orthogneiss, mylonite and non-coaxial deformation of granites: the example of the South Amorican Shear Zone: Journal of Structural Geology, v. 1, p. 31-42.

Buck, W.R., 1988, Flexural rotation of normal faults: Tectonics, v. 7, p. 959-973.

Crittenden, M.D., Jr., Coney, P.J., and Davis, G.H., eds., 1980, Cordilleran metamorphic core complexes: Geological Society of America Memoir 153, 490 p.

Davis, G.A., and G.S. Lister, 1988, Detachment faulting in continental extension; Perspectives from the southwestern U.S. Cordillera, *in* Clark, S.P., Jr., Burchfiel, B.C., and Suppe, J., eds., Processes in continental lithosphere deformation: Geological Society of America Special Paper 218, p. 133-160.

Davis, G.A., Lister, G. S., and Reynolds, S. J., 1986, Structural evolution of the Whipple and South Mountains shear zones, southwestern United States: Geology, v. 14, p. 7-10.

Davis, G.H., 1980, Structural characteristics of metamorphic core complexes, southern Arizona, *in* Crittenden, M.D., Jr., Coney, P.J., and Davis, G.H., eds., Cordilleran metamorphic core complexes: Geological Society of America Memoir 153, p. 35-77.

Dickinson, W.R., 1991, Tectonic setting of faulted Tertiary strata associated with the Catalina core complex in southern Arizona: Geological Society of America, Special Paper 264, 106 p.

Drewes, H., 1977, Geologic map and sections of the Rincon Valley Quadrangle, Pima County, Arizona: U.S. Geological Survey Miscellaneous Investigations Series Map I-997, scale 1:48,000.

Force, E.R., 1997, Geology and mineral resources of the Santa Catalina Mountains, southeastern Arizona: Tucson, Arizona, Center for Mineral Resources, Monographs in Mineral Resource Science, n. 1, 134 p.

Hanmer, S., and Passchier, C., 1991, Shear-sense indicators: A review: Geological Survey of Canada Paper 90-17, 72 p.

Keith, S. B., Reynolds, S. J., Damon, P. E., Shafiqullah, M., Livingston, D. E., and Pushkar, P. D., 1980, Evidence for multiple intrusion and deformation within the Santa Catalina-Rincon-Tortolita crystalline complex, southeastern Arizona, *in* Crittenden, M.D., Jr., Coney, P.J., and Davis, G.H., eds., Cordilleran metamorphic core complexes: Geological Society of America Memoir 153, p. 217-267.

Kruse, S., McNutt, M., Phipps-Morgan, J., Royden, L., and Wernicke, B., 1991, Lithospheric extension near Lake Mead, Nevada: A model for ductile flow in the lower crust: Journal of Geophysical Research, v. 96, p. 4435-4456.

Lister, G.S., and Snoke, A.W., 1984, S-C mylonites: Journal of Structural Geology, v. 6, p. 617-638.

Mawer, C.K., 1987, Shear criteria in the Grenville Province, Ontario, Canada: Journal of Structural Geology, v. 9, n. 5/6, p. 531-539.

Naruk, S.J., 1987, Displacement calculations across a metamorphic core complex mylonite zone: Pinaleño Mountains, southeastern Arizona: Geology, v. 15, no. 7, p. 656-660.

Naruk, S.J., and Bykerk-Kauffman, A., 1990, Late Cretaceous and Tertiary deformation of the Santa Catalina metamorphic core complex, Arizona, *in* Gehrels, G.E., and Spencer, J.E., eds., Geologic excursions through the Sonoran Desert region, Arizona and Sonora: Arizona Geological Survey Special Paper 7, p. 41-50.

Pain, C.F., 1985, Cordilleran metamorphic core complexes in Arizona: A contribution from geomorphology: Geology, v. 13, p. 871-874.

Reynolds, S.J., and Lister, G.S., 1990, Folding of mylonitic zones in Cordilleran metamorphic core complexes: Evidence from near the mylonitic front: Geology, v. 18, no. 3, p. 216-219.

Simpson, C., and Schmid, S.M., 1983, An evaluation of criteria to deduce the sense of movement in sheared rocks: Geological Society of America Bulletin, v. 94, no. 11, p. 1281-1288.

Smith, B.M., Reynolds, S.J., Day, H.W., and Bodnar, R., 1991., Deep-seated fluid involvement in ductile-brittle deformation and mineralization, South Mountains metamorphic core complex, Arizona: Geological Society of America Bulletin, v. 103, p. 559-569.

Spencer, J.E., 1984, Role of tectonic denudation in warping and uplift of low-angle normal faults: Geology, v. 12, p. 95-98.

Spencer, J.E., 1999, Geologic continuous casting below continental and deep-sea detachment faults and at the striated extrusion of Sacsayhuamán, Peru: Geology, v. 27, p. 327-330.

Spencer, J.E., 2000, Possible origin and significance of extension-parallel drainages in Arizona's metamorphic core complexes: Geological Society of America Bulletin, v. 112, p. 727-735.

Wernicke, B., 1990, The fluid crustal layer and its implications for continental dynamics, *in* Salisbury, M., and Fountain, D.M., eds., Exposed cross sections of the continental crust: Dordrecht, Holland, Kluwer Academic Publishers, p. 509-544.

Wernicke, B., 1992, Cenozoic extensional tectonics of the U.S. Cordillera, *in* Burchfiel, B.C., Lipman, P.W., and Zoback, M.L., eds., The Cordilleran Orogen: Coterminous U.S.: Boulder, Colorado, Geological Society of America, The Geology of North America, v. G-3, p. 553-581.

Wernicke, B., and Axen, G.J., 1988, On the role of isostasy in the evolution of normal fault systems: Geology, v. 16, p. 848-851.

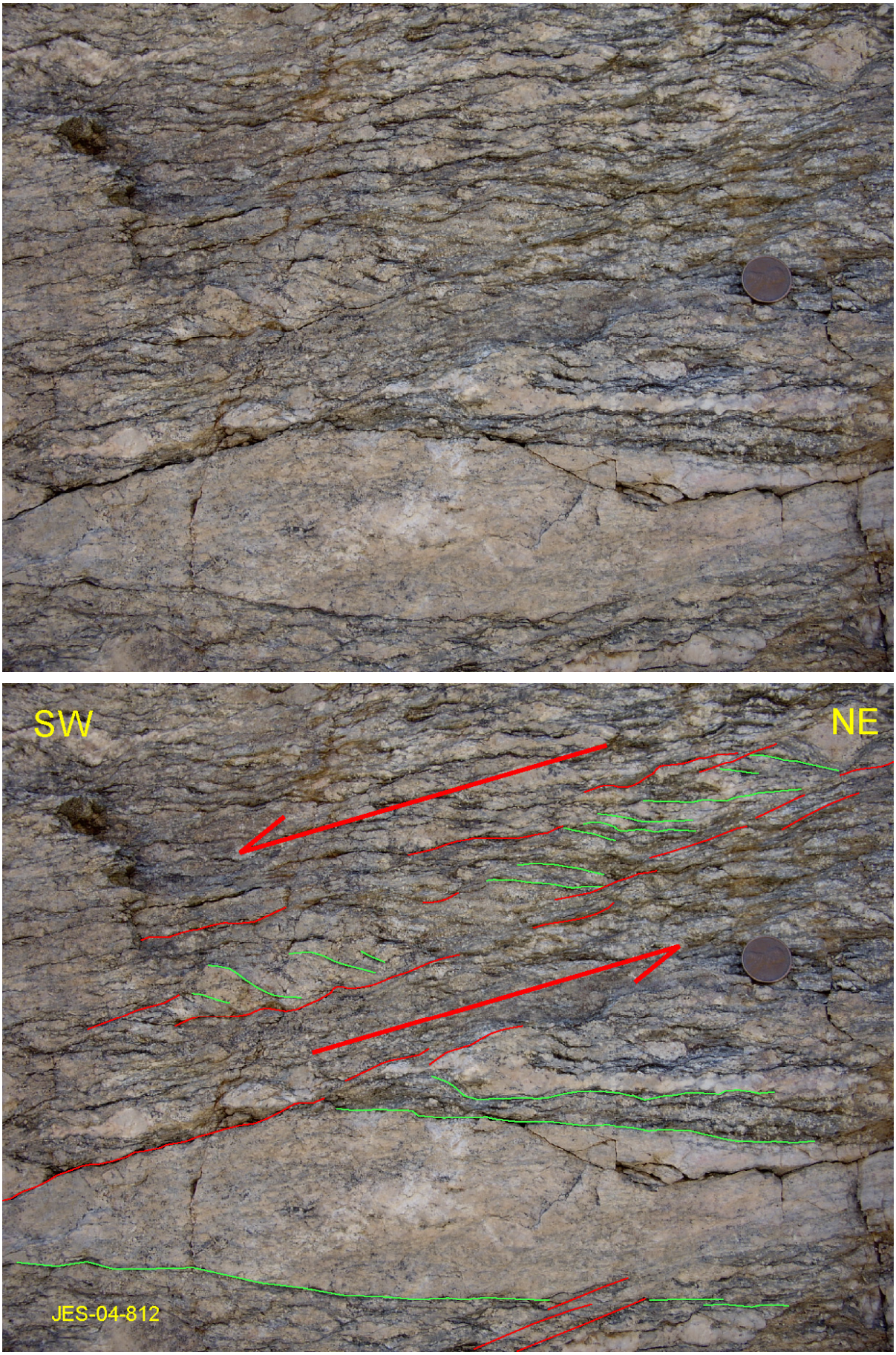

Figure 3. S surfaces (flattening, in green) and C surfaces (shearing, in red) in S-C mylonite.

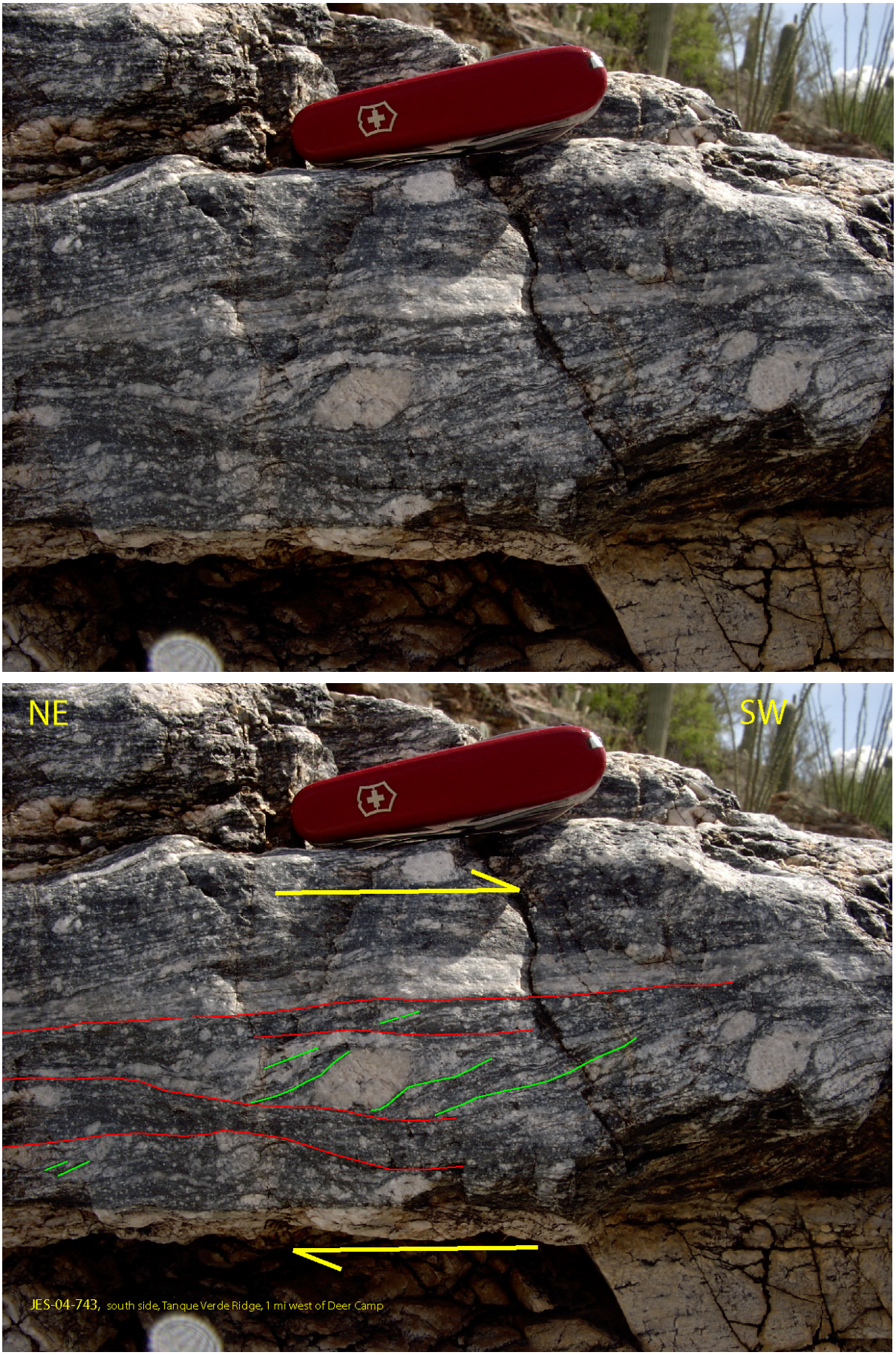

Figure 4. S surfaces (flattening, in green) and C surfaces (shearing, in red) in S-C mylonite.

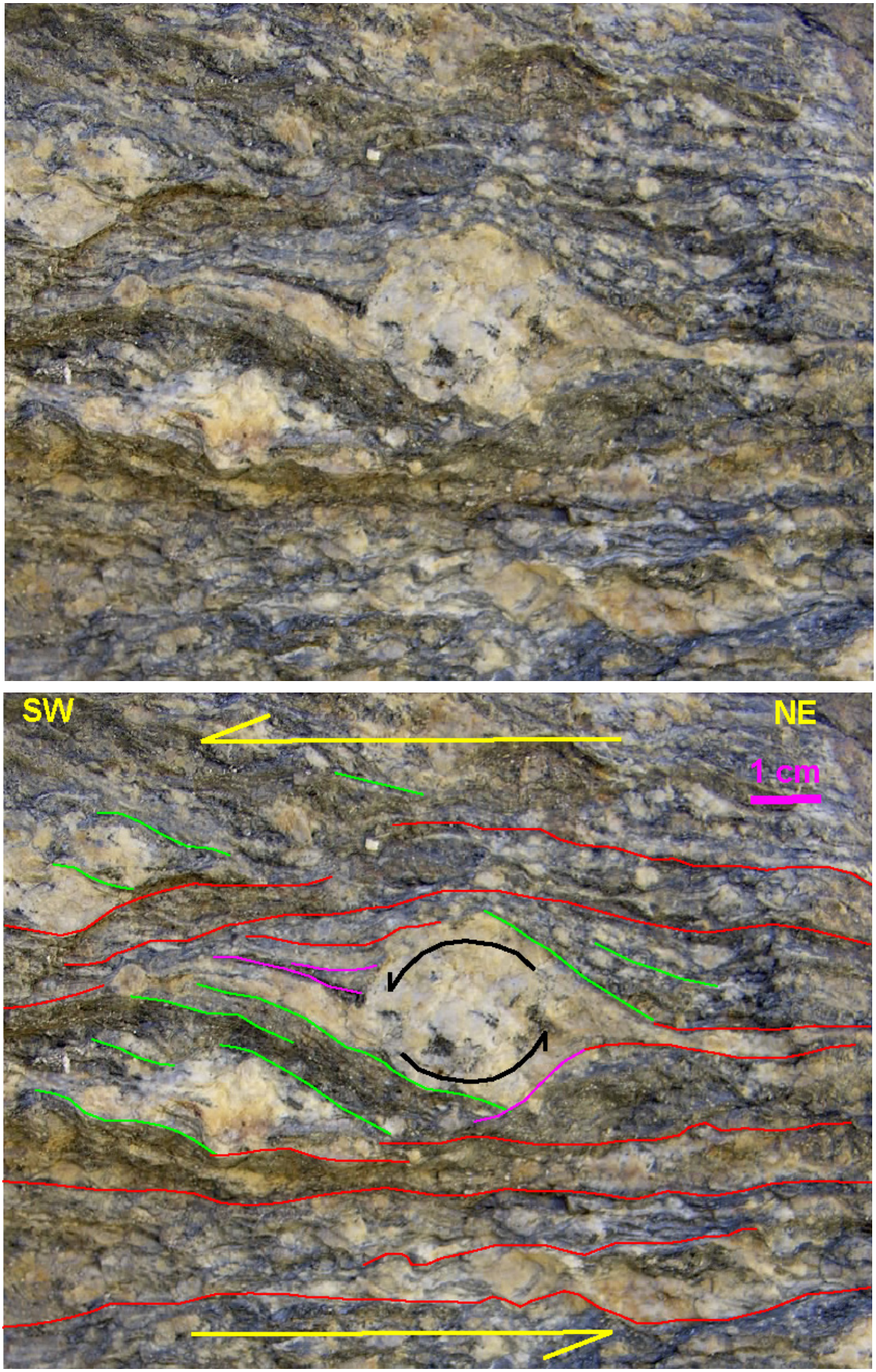

Figure 5. Rotated porphyroclast in S-C mylonite. S surfaces (flattening, in green), C surfaces (shearing, in red), and possible C surfaces rotated with porphyroclast and shielded by porphyroclast from further shearing (purple).

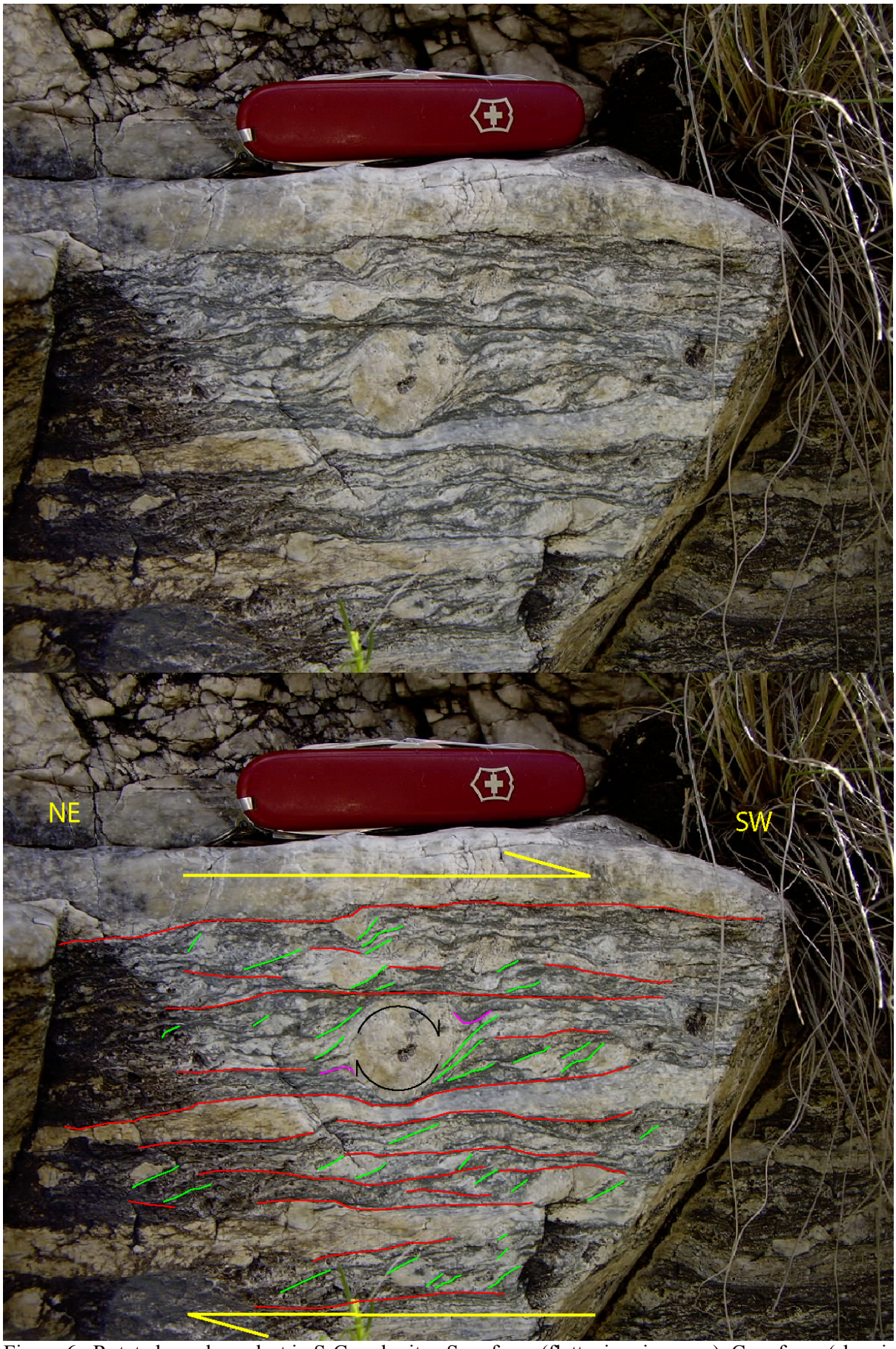

Figure 6. Rotated porphyroclast in S-C mylonite. S surfaces (flattening, in green), C surfaces (shearing, in red), and possible C surfaces rotated with porphyroclast and shielded by porphyroclast from further shearing (purple).

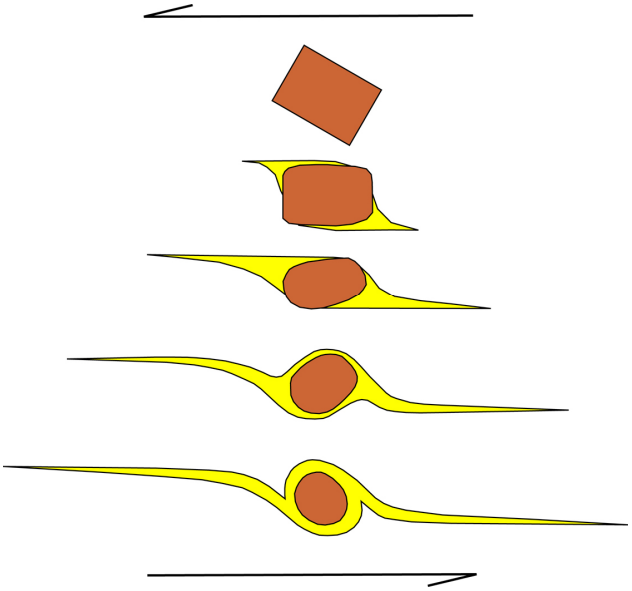

Figure 7. Rectangular K-feldspar megacryst modified by shearing in a top-left shear zone. Idealized development of asymmetric tails on a slightly to moderately rounded porphyroclast is followed by rotation of well-rounded porphyroclast (modified from Mawer, 1987). The crushed corners of the megacryst make up the tails.

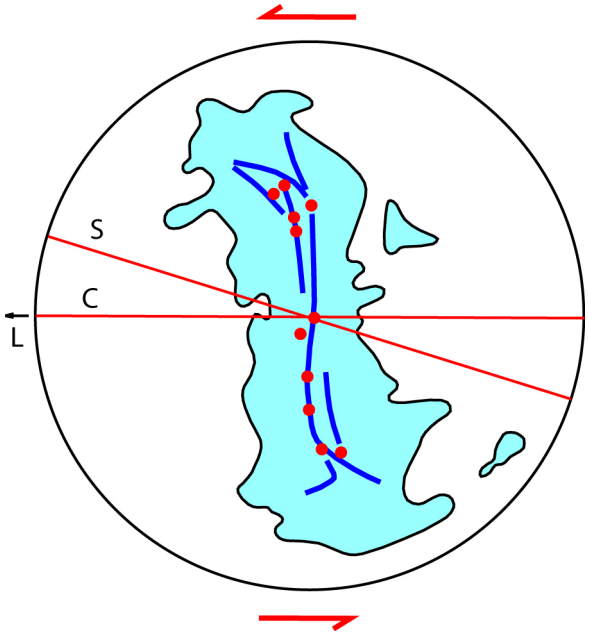

Figure 8. Synoptic lower-hemisphere projection of quartz c-axes. Dots are maximum orientations of individual diagrams. Modified from Davis et al. (1987)

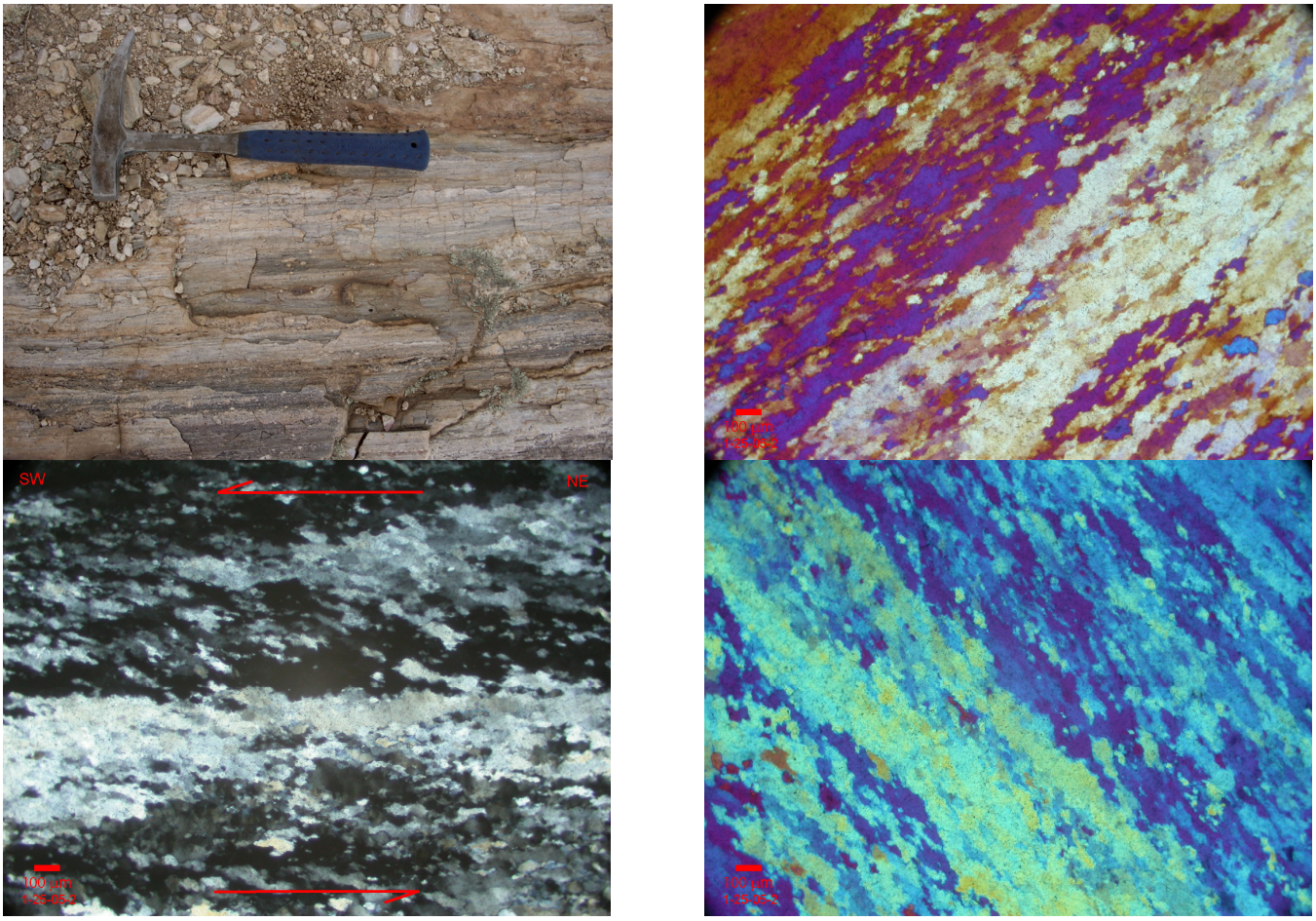

Figure 9 A-D. (A) Outcrop of highly strained quartz vein with well developed lineation and severe grain size reduction. (B) Photomicrograph (with polarized light) of highly strained quartz vein, section oriented parallel to lineation and perpendicular to foliation. Foliation orientation is apparent, as are elongate quartz subgrains inclined to left and suggesting top-left shearing. (C, D) As in (B) but with quartz plate inserted and stage rotated, showing dominant yellow and orange for subtractive birefringence from quartz crystals and quartz plate, and dominant blue for additive birefringence. This optical contrast for different microscope stage positions reveals strong preferred c-axis orientation of quartz grains.

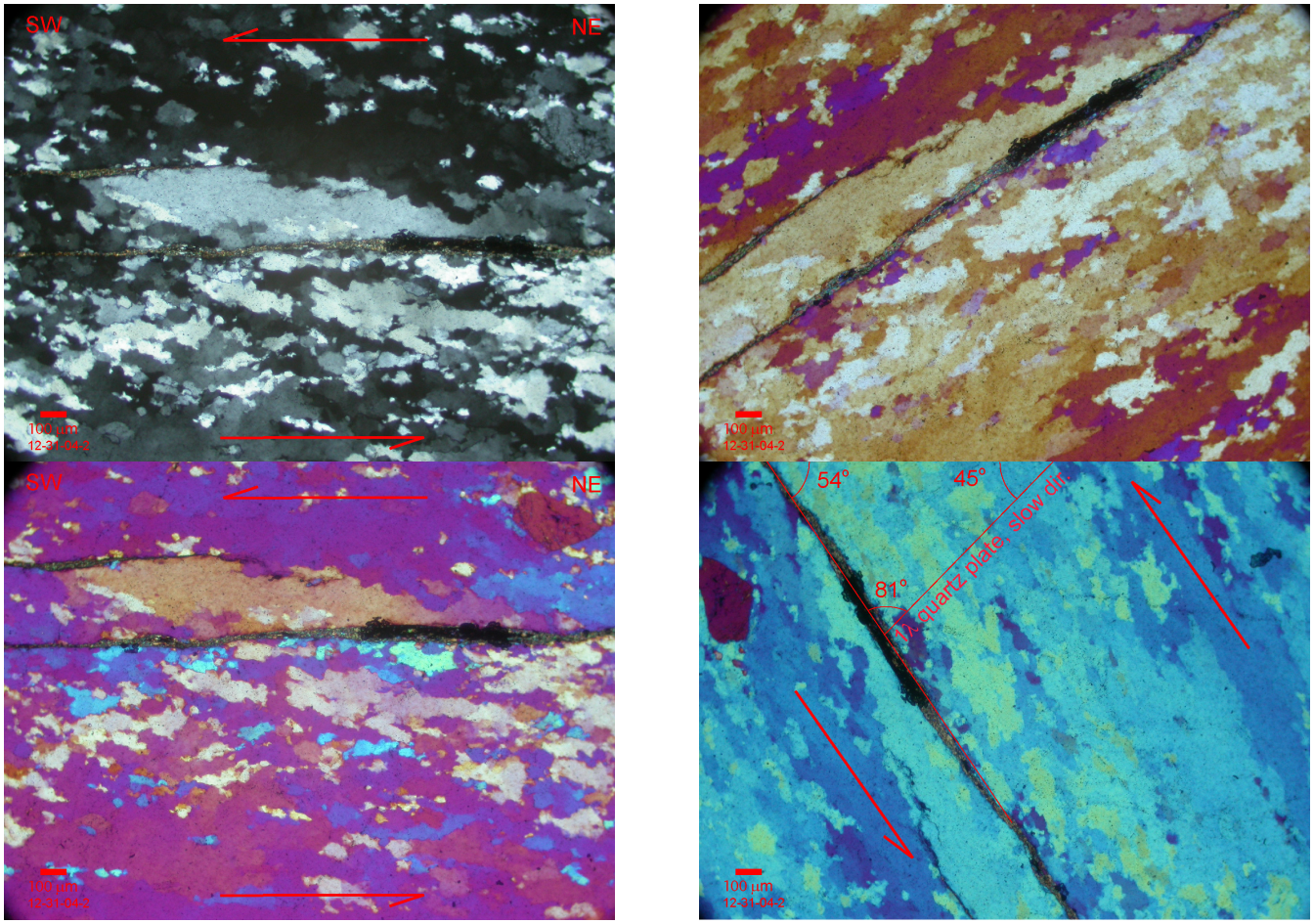

Figure 9 E-H. (E) Photomicrograph (with polarized light) showing thin zone of highly comminuted mica, across center of photomicrograph, that helps define foliation plane within fine grain, recrystallized quartz. (F) As in (E) but with quartz plate inserted. (G, H) As in (F) but with stage rotated to show maximum additive birefringence from quartz crystals and quartz plate (blue) and minimum subtractive birefringence (yellow and orange). With the thin linear crushed zone of highly comminuted mica it is possible to measure angular discordance between statistical preferred orientation of c-axes in quartz and shear surface (C surface in S-C mylonite). In (G) this discordance is 81°, which indicates that quartz c-axes are tilted to the left and indicate a top-left sense of shear, as do the elongate quartz subgrains.

FIELD GUIDE TO THE FORERANGE ARCH

Catalina Highway begins at its intersection with Tanque Verde Road, a major east-west road in the northwestern Tucson basin. Drive to Tanque Verde Road and turn north (left if you are headed east) on Catalina Highway. Catalina Highway veers northeast and you will approach the foot of the Santa Catalina Mountains in a straight line. At the foot of the range the highway crosses the buried Catalina detachment fault. Sparse hematite-stained fractures are more abundant at the lowest bedrock exposures at the very foot of the range than farther up the highway (these were identified within a hundred meters of the highway to the west). These are probably the consequence of fracturing and fluid entry during faulting and exhumation of warm footwall rocks.

The highway enters the mouth of Soldier Canyon at the foot of the range. Here you will see the visually striking banded mylonitic gneiss that makes up much of the Catalina Forerange. The dark rocks with 1 to 4 cm augen are most likely foliated Oracle Granite, which is undeformed at the north end of the Santa Catalina Mountains around the town of Oracle. This is one of the so-called anorogenic granites that were intruded in a belt across North America at about 1.4 Ga. These granites typically have very few pegmatites and quartz veins (Anderson, 1989), but here the foliated and gneissic granite is intruded by numerous pegmatites, quartz veinlets, and leucogranite sills which have been dated at 40-50 Ma (Eocene). (A leucogranite is a light colored granite with a low percentage of mafic minerals). The layered suit of igneous rocks visible along the highway here is known as the forerange gneiss, after the Catalina forerange which forms the southwestern part of the Santa Catalina Mountains.

This gneiss is overprinted by a mylonitic fabric that is generally parallel to lithologic layering in the gneiss but is difficult to distinguish from the gneissic in many outcrops. The mylonitic fabric is most readily identified on surfaces parallel to lithologic layering where the associated mylonitic lineation is visible. Feldspar augen and highly sheared quartz and mica are visible on surfaces parallel to lineation and perpendicular to foliation, and with careful search and study one can commonly find shear-sense indicators on such surfaces.

The Babad Do'ag area is on the south side of the forerange arch, which is an east-west trending antiformal culmination of gneissic layering and mylonitic foliation (see also Force, 1997). Top-southwest shear-sense indicators are common on the south side of the arch, whereas at stops 2 and 3 on the north side of the forerange arch, top northeast are dominant (see also Naruk and Bykerk-Kauffman, 1990; Reynolds and Lister, 1990). My interpretation of the origin of the forerange arch is presented below after description of highway stops 1, 2, and 3.

Highway Stop #1: Babad Do'ag overlook. Stop at the Babad Do'ag overlook parking area about two miles up the highway. (The Tohono O'odham name means "Frog Mountain"). The rock wall on the south side of the parking lot provides a good display of the diverse granitic, gneissic, and mylonitic rocks that make up the area. The lineations associated with the mylonitic fabric are well displayed on the northwest edge of the parking lot on a small ridge between the parking lot and the highway. These lineations generally trend about 245° and plunge obliquely southwestward across the south-facing range front.

After looking at the rock collection in the wall and the lineation on the northwest side of the parking lot, proceed to the Babad Do'ag trailhead, which is located across the highway and a few tens of meters east of the parking lot entrance. Be careful crossing the highway at this curve as visibility is especially poor for cars and bicycles traveling down the highway. The bicyclists may travel as fast as the cars but are much quieter. Several interesting features are visible along the trail north of the highway.

Figure 10 (next page). Map of lower Catalina Highway area and the Babad Do'ag area, showing location of field stops, axis of forerange arch, and lineation and foliation symbols. Green lineation symbols – top southwest; orange – top northeast.

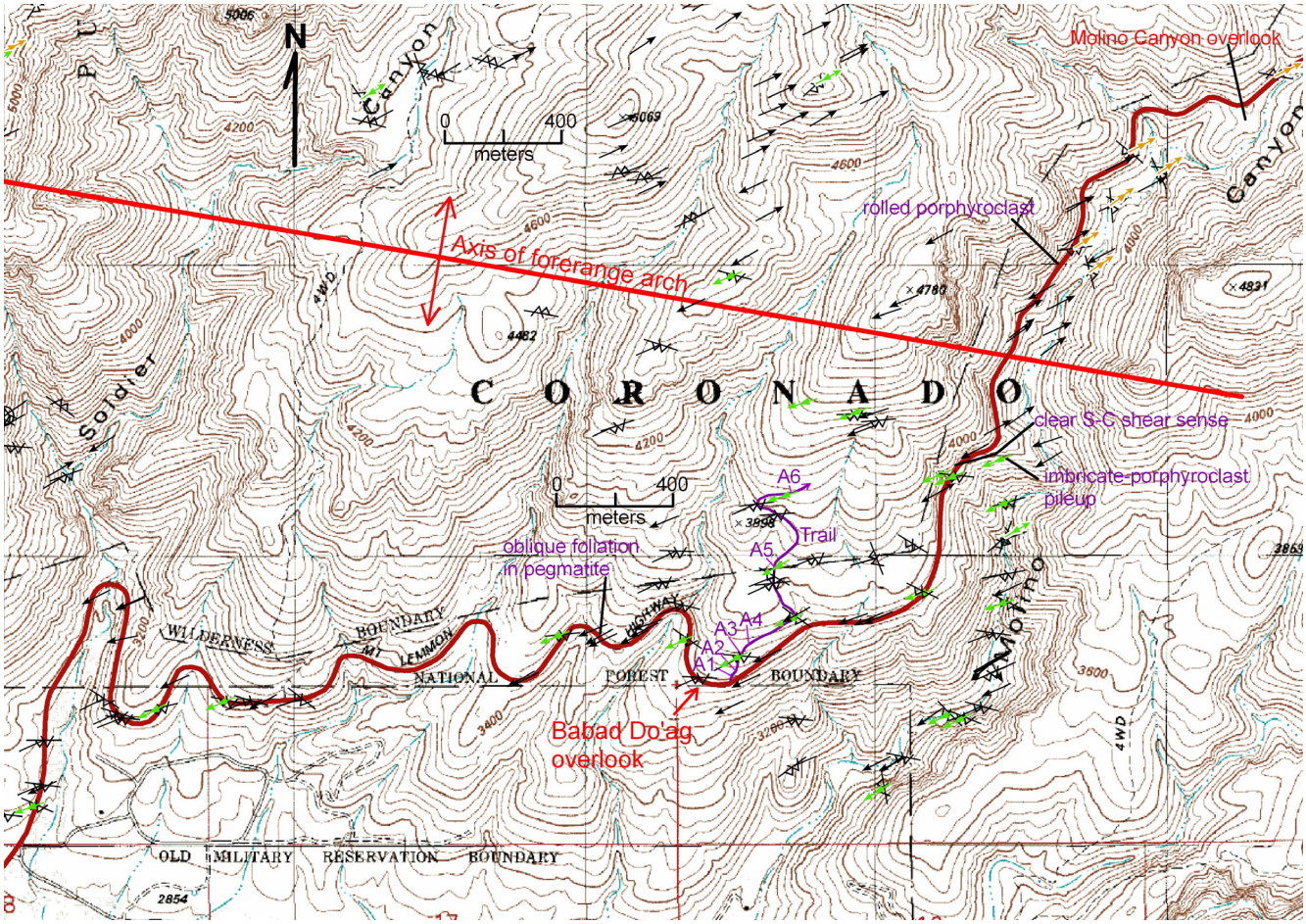
N
0
400
meters
Axis of forerange arch
Molino Canyon overlook
rolled porphyroclast
C O R O N A D O
clear S-C shear sense
imbricate-porphyroclast pileup
A6
Trail
A5
A4
A3
A2
A1
oblique foliation in pegmatite
Babad Do'ag overlook
WILDERNESS
BOUNDARY
MT LEMMON
NATIONAL
FOREST
BOUNDARY
HIGHWAY
OLD MILITARY RESERVATION BOUNDARY
Soldier
Canyon
4WD

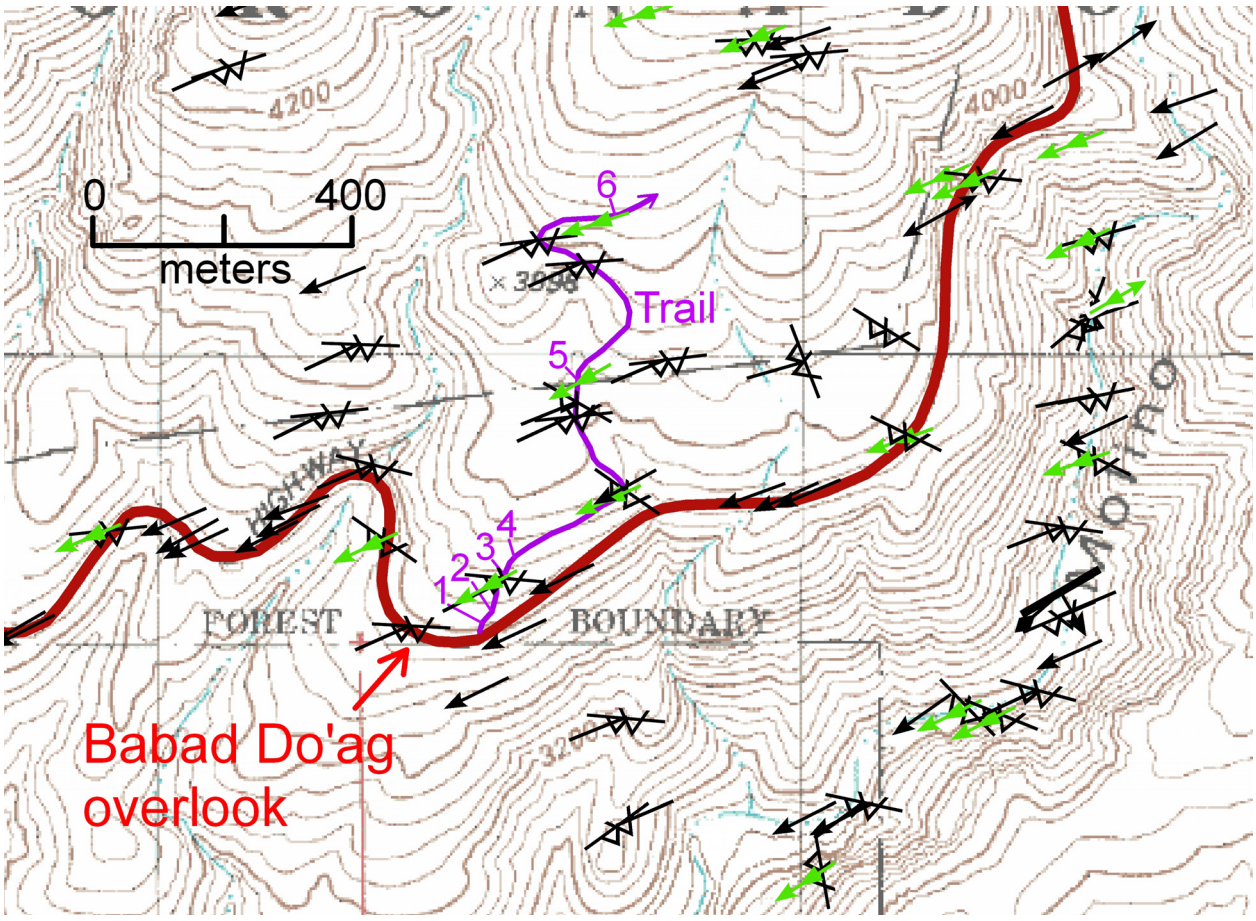
0
400
meters
6
Trail
5
4
3
2
1
HIGHWAY
FOREST
BOUNDARY
Babad Do'ag overlook

Table 1: Babad Do'ag field stops				
Field Stop No.	UTME*	UTMN*	Feature	Station
A1	526503	3574580	porphyroclasts	JES-05-233
A2	526521	3574596	lineated mylonitic quartz veinlet	JES-05-234
A3	526539	3574650	top-southwest shear-sense indicator	JES-05-236
A4	526556	3574679	undulating mylonitic shear surface	JES-05-237
A5	526655	3574952	undulating mylonitic shear surface	JES-05-241
A6	526711	3575207	top-southwest shear-sense indicator	JES-05-243
*NAD 27, zone 12				

A1: Highly sheared, dark, porphyritic granite is well exposed approximately 20 to 30 meters along the trail from the Babad Do'ag trailhead. Mylonitic shearing has caused brittle rounding of K-feldspar phenocrysts which would now be termed "porphyroclasts." Strongly developed lineation reveals shearing direction. The protolith of foliated dark granite is probably the 1.4 Ga Oracle Granite.

A2: At this stop the trail crosses a strongly lineated quartz veinlet oriented parallel to mylonitic foliation. Such veinlets probably became sites of concentrated shear strain as cooling increased rock strength just before transition to brittle faulting. Under these conditions feldspar-bearing host rocks are significantly stronger that quartz veins, which deform by the crystal-plastic deformation mechanisms of dislocation propagation and grain-boundary diffusion while feldspathic host rocks have largely or completely entered the brittle deformation regime.

In thin section, these highly sheared quartz veinlets appear as 30 to 60 μm (10^{-6} m) quartz subgrains that have sutured, irregular boundaries with adjacent quartz subgrains. Elongate areas of hundreds of quartz subgrains all appear to have similar but slightly different orientations. Grain-size reduction in these rocks was extreme. If, for example, a 4 mm diameter quartz grain was transformed into a sutured aggregate of 40 μm quartz subgrains (with similar but not identical crystallographic orientation), then this 4 mm quartz grain would have been broken into a million subgrains. Because the grains are sutured and not separated by brittle slip surfaces, the process of grain-size reduction must have occurred in a transitional regime of semi-brittle, semi-ductile deformation. It may be the last type of crystal-plastic deformation to occur before complete transition to brittle faulting and fracturing during exhumation and cooling of the detachment-fault footwall.

A3: Here the trail crosses a typical mix of foliated, dark, porphyritic granite and medium- to fine-grained leucogranite, both mylonitized and lineated. On a ledge on the uphill side of the trail is a mediocre top-southwest shear-sense indicator in S-C mylonite.

A4: Here the trail crosses a mylonitic shear surface that has irregularities in it. For these irregularities to survive mylonitic shearing, the rocks above the bumps must have flowed up and over the bumps, which suggests that the rock was sufficiently soft during mylonitization that it could flow over such irregularities.

A5: Slightly to east of the trail, a highly sheared quartz vein forms part of an exposed surface that is parallel to mylonitic foliation. Irregularities in surface suggest, as at A4, that rocks were sufficiently soft that they could flow over bumps in the shear zone during mylonitization.

A6: A very well displayed, top-southwest, S-C shear-sense indicator is exposed along the side of the trail (Figure 11). An approximately 100-meter length of trail here has very well developed lineation in dark, porphyroclastic granite and fine grained leucogranite.

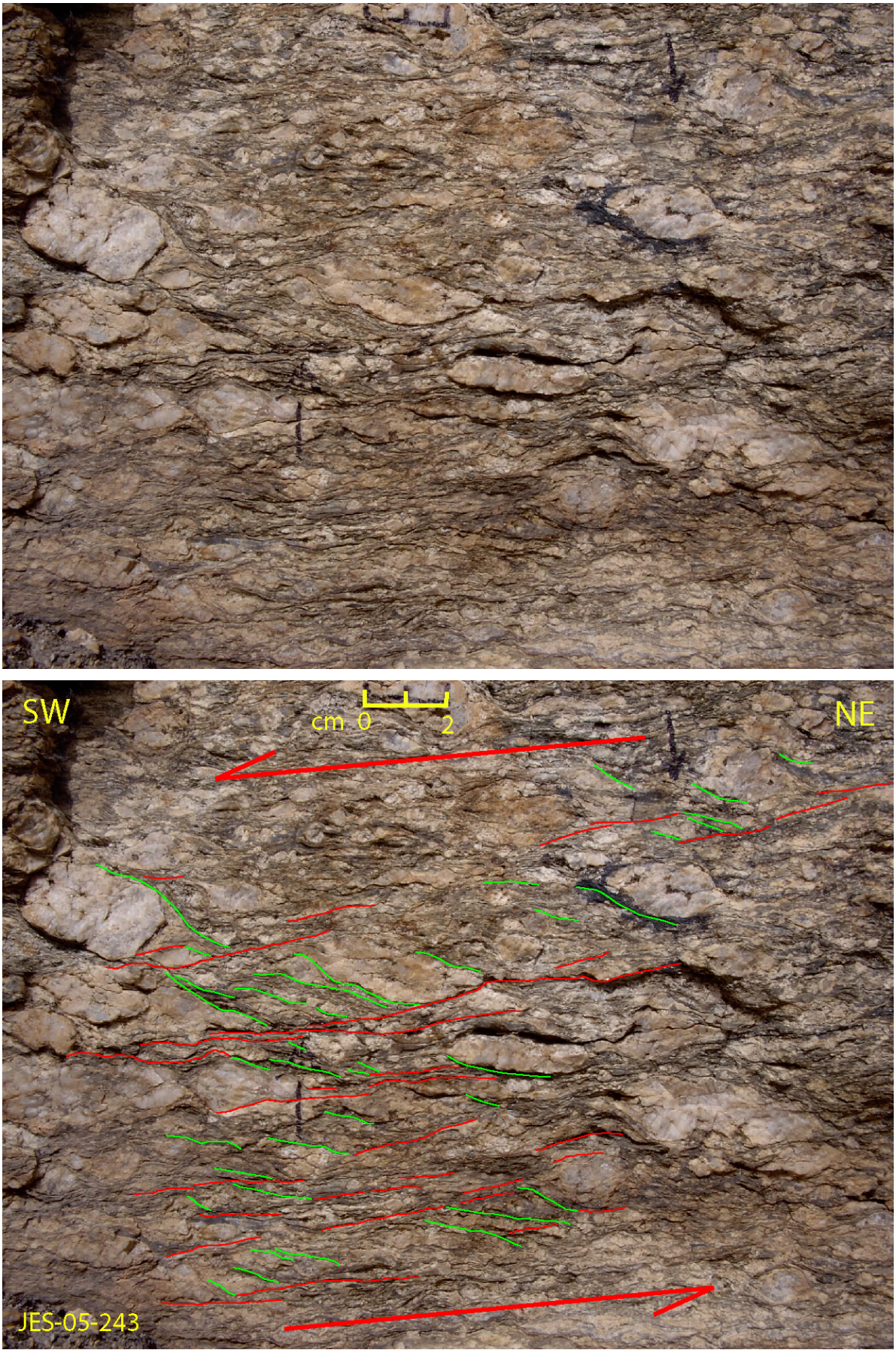

Figure 11. S-C mylonite at stop A6. S surfaces highlighted in green, C in red.

Highway Stop #2: Molino Basin: Drive approximately 3 miles up the Catalina Highway from the Babad Do'ag overlook to Molino Basin. At about 1 mile up the road you will cross the axis of the forerange arch. At Molino Basin, turn left into the picnic area and campground entrance and park in the parking area around the restroom building at the entrance. You will need to walk across the highway to hike up Molino Canyon. Be careful here as cars travel fast and visibility is not great.

The walk up Molino Canyon provides an opportunity to view the north-dipping side of the forerange arch. Lithologic layering in the weakly layered to gneissic granitic rocks is the result of Eocene intrusion of sheets of granite and pegmatite between sheets of Eocene and older granite, and associated high temperature flattening (e.g., Force, 1997). The younger mylonitic fabric varies in development so that some areas are undeformed or weakly deformed, other areas are moderately affected by mylonitization over shear-zone thicknesses of 1 to 10 meters, and a few strongly mylonitized zones are centimeters to tens of centimeters thick. Top-northeast shear-sense indicators were identified at four points along the canyon (Table 2; Figure 12). Although these indicators are subtle, my identification of top-northeast shear in this canyon was confirmed on field trips with structural geologists Chuck (Christopher) Bailey (College of William and Mary, Virginia) and Sharon Mosher (University of Texas, Austin), and is consistent with previous recognition of top-northeast shear indicators in this area by Naruk and Bykerk-Kauffman (1990) and Reynolds and Lister (1990).

It is a scenic hike up the canyon, partially on a trail and partially within the wash. When the wash is running, generally during and after heavy winter rains or summer thunderstorms, a small waterfall about 1 km up the canyon (where the wash crosses the 4600 foot contour) is active and the wet, polished rocks next to the waterfall clearly reveal a shear zone within the granite. A steep, unofficial trail extends around the west side of the waterfall.

Table 2: Molino Basin field stops

Field Stop No.	UTME*	UTMN*	Feature	Station
B1	529682	3579012	top-northeast shear-sense indicator	JES-04-753
B2	529767	3577999	top-northeast shear-sense indicator	JES-04-754
B3	529775	3578350	top-northeast shear-sense indicator	JES-04-757
B4	530209	3578677	top-northeast shear-sense indicator	JES-04-763

**NAD 27, zone 12*

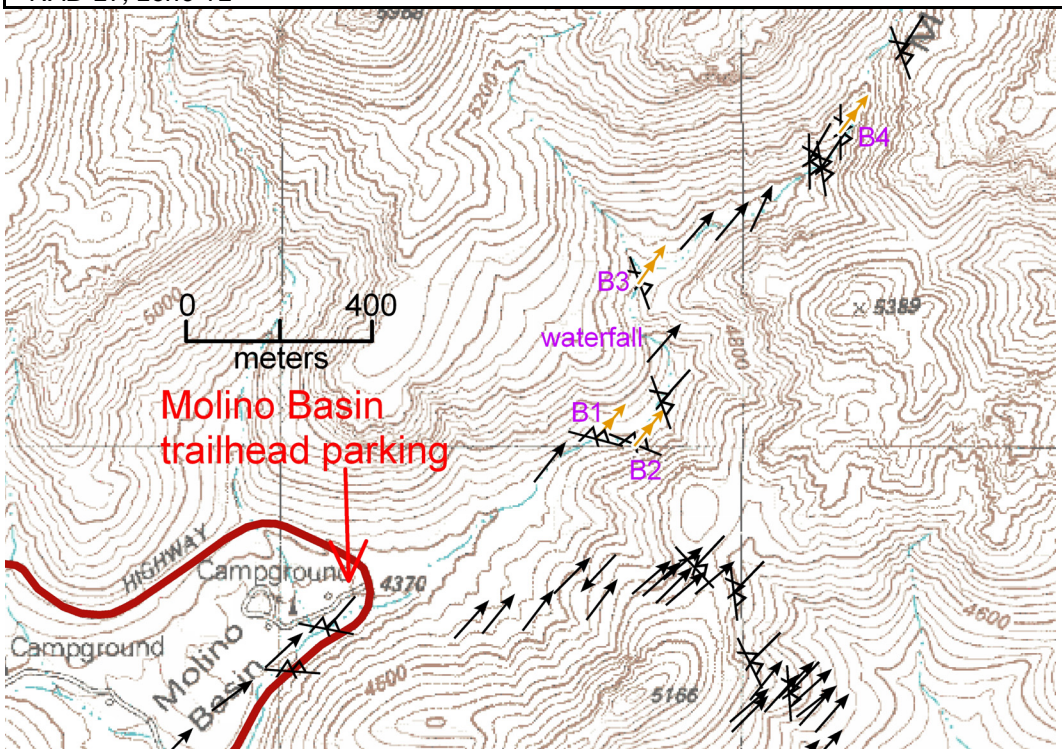

Highway Stop #3: Prison Camp and Gordon Hirabayashi Recreation Area. A trail leading southwest from the Prison Camp parking lot forks at about 350 meters from the trailhead (Figure 13). The left fork continues down Soldier Canyon and reaches the Catalina Highway below Babad Do'ag. Take the right fork, which follows a relict dirt road to Sycamore reservoir (now filled with sand). After crossing Soldier Creek on a small bridge, walk 100-150 m up the trail until you see a small gulch on the left that extends uphill to the west-southwest from the wash and trail. This gulch contains numerous top-northeast, S-C mylonite, shear-sense indicators, and is the best collection of such indicators that I know of on the north side of the forerange arch (Table 3; Figures 13, 14, 15). Use the map or table below to find the shear-sense indicators, or find others in the same general area. The purpose of visiting this area is simply to identify these shear-sense indicators and convince yourself that, in fact, shear sense is top-northeast, opposite to that at Babad Do'ag and other areas on the south side of the forerange arch. At stop C8, coarse, feldspathic pegmatites appear to cut across mylonitic fabric. However, there is significant ambiguity concerning whether the pegmatites are post-mylonitic or pre- to syn-mylonitic. The pegmatites contain so little quartz and such coarse and abundant feldspar that they might be pre-mylonitic but effectively resisted mylonitic deformation and so appear to be post-mylonitic.

Table 3: Prison Camp field stops

Field Stop No.	UTME*	UTMN*	Feature	Station
C1	525998	3577441	top-northeast shear-sense indicator	JES-05-133
C2	525895	3577413	top-northeast shear-sense indicator	JES-05-134
C3	525878	3577405	top-northeast shear-sense indicator	JES-05-135
C4	525697	3577406	top-northeast shear-sense indicator	JES-05-137
C5	525605	3577407	top-northeast shear-sense indicator	JES-05-138
C6	525158	3577442	top-northeast shear-sense indicator	JES-05-143
C7	525083	3577358	top-northeast shear-sense indicator	JES-05-145
C8	524446	3577068	syn-deformation(?) pegmatites	JES-05-181

**NAD 27, zone 12*

Historical Note – Prison Camp and Gordon Hirabayashi: A Coronado National Forest web page states the following about the Federal prison camp located at this site from 1937 until the camp was torn down in the 1970s: All of the prisoners at the honor camp had been convicted of Federal crimes, ranging from immigration law violations to tax evasion to bank robbery. During World War II, many of the prisoners at the honor camp were conscientious objectors, including Jehovah's Witnesses and Hopi Indians whose religions prohibited them from serving in the military. Some of the prisoners were Japanese-Americans protesting forced relocation during World War II. The "honor camp" designation reflects the lack of fences, walls, or armed guards. The Prison Camp was built here so that prisoners would do most of the labor to build the Catalina Highway.

In 1942, Gordon Hirabayashi was a senior at the University of Washington in Seattle. Instead of reporting for relocation, as mandated by the Federal Government in 1942 for citizens of Japanese descent, Hirabayashi turned himself in to the FBI. He challenged the constitutionality of internment based solely on race or ancestry and openly refused to comply with the relocation order. His case went all the way to the Supreme Court, but Hirabayashi was convicted. In a landmark decision in American judicial history, the court ruled that racial discrimination by the government was constitutional in a wartime emergency. Because the Federal Attorney would not provide transportation, Hirabayashi hitchhiked alone from Spokane, Washingtion, to Tucson to serve his sentence at the Federal honor camp in the Santa Catalina Mountains. In 1999, the Coronado National Forest named this site after its most famous inmate, Dr. Gordon Hirabayashi, who participated in the dedication ceremony.

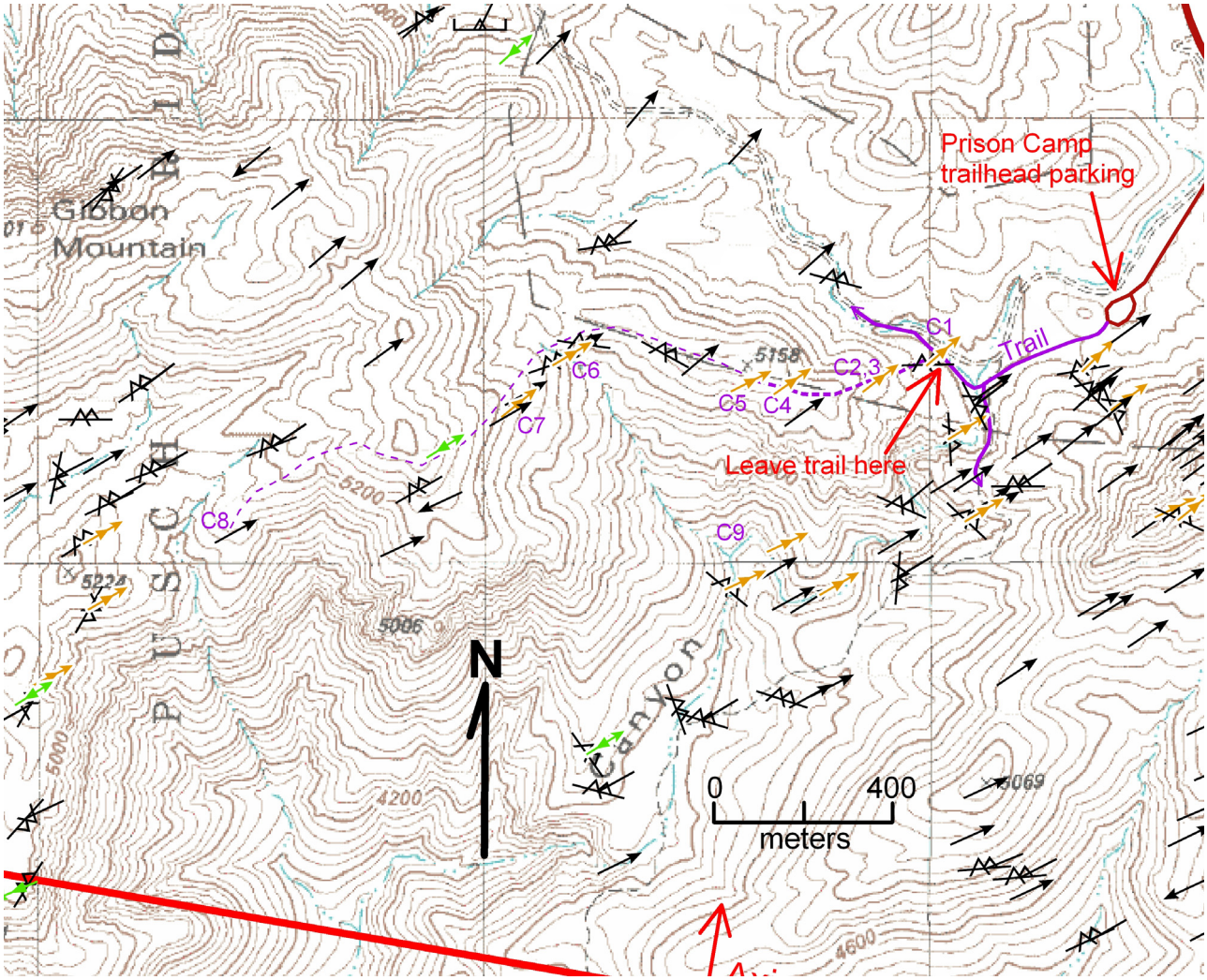

Figure 13. Map of Prison Camp area, showing location of field stops, axis of forerange arch, and lineation and foliation symbols. Green lineation symbols – top southwest; orange – top northeast.

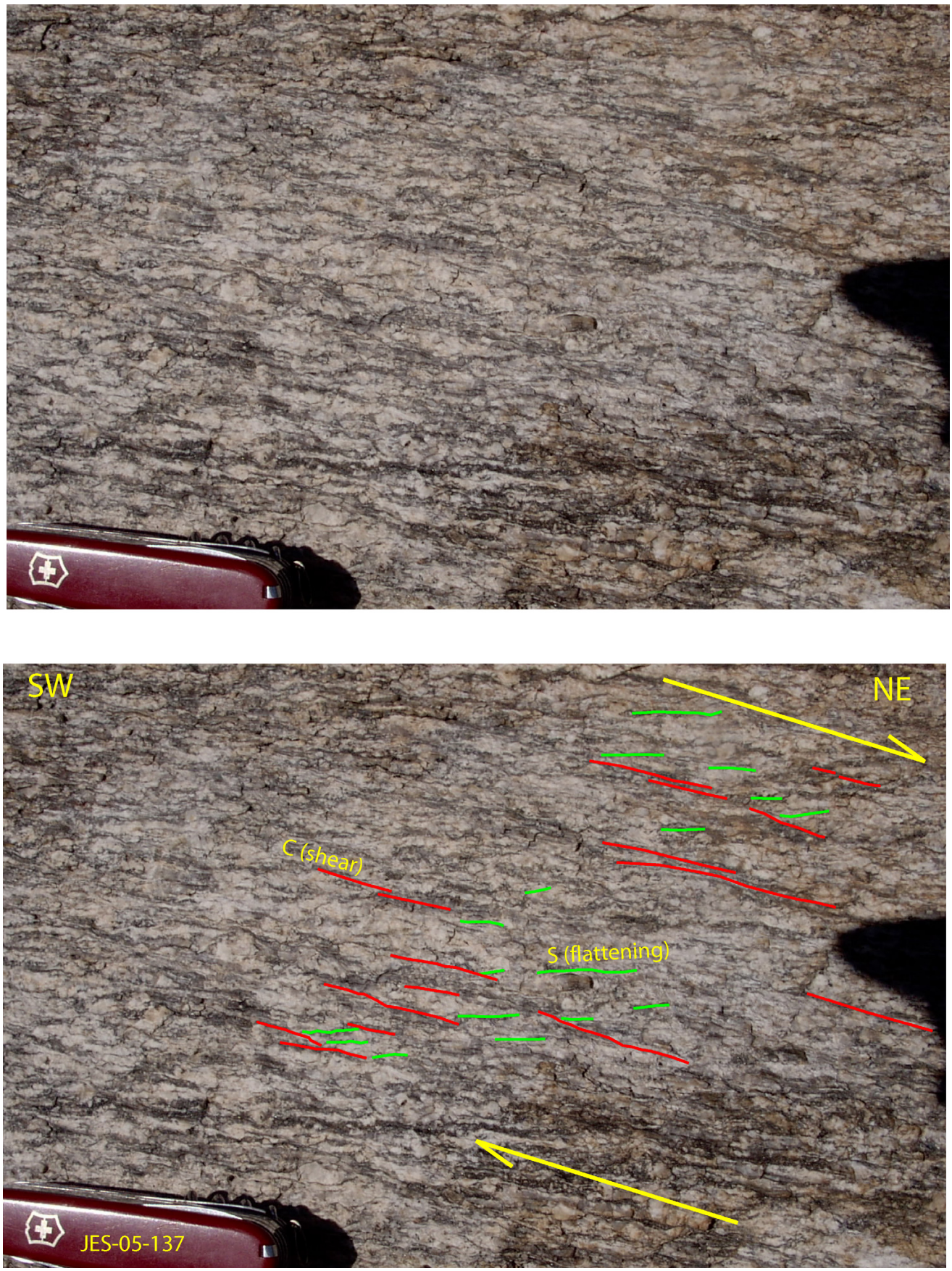

Figure 14. S-C mylonite at field-stop C4.

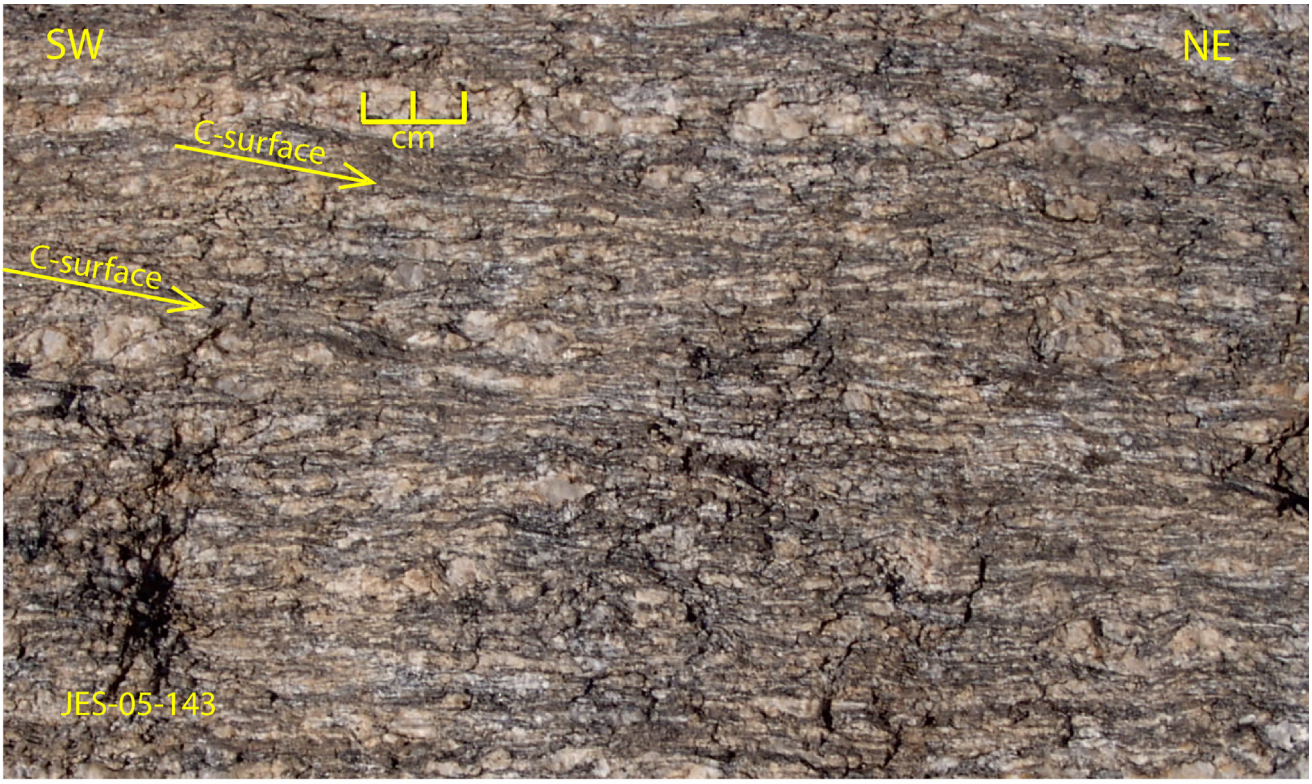

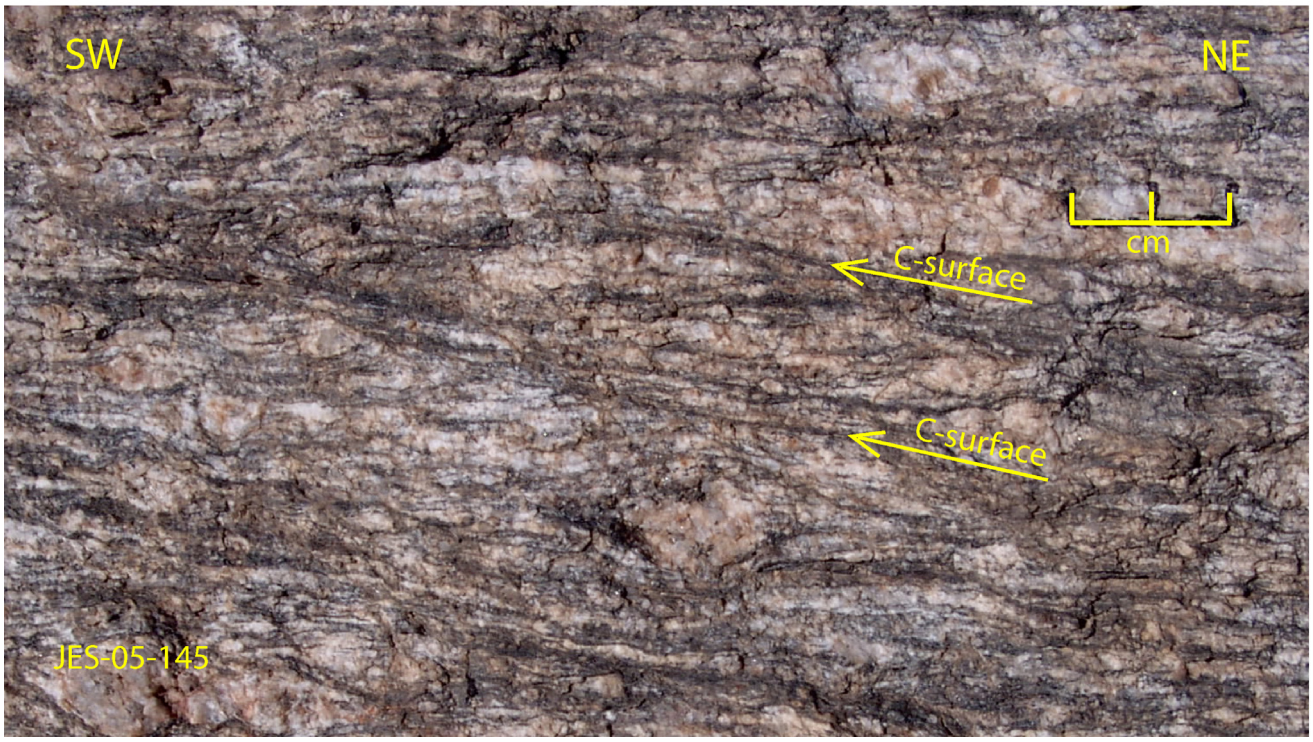

Figure 15. S-C mylonite at field-stops C6 and C7.

The Forerange Arch

The east-west trending forerange arch is the dominant structural feature of the Catalina forerange. It is represented by an antiformal culmination of lithologically layered gneiss and mylonitic foliation that extends from the Sabino Canyon area to east of Molino Creek with an axial trend of 100° (S 80° E). The most striking and controversial characteristic of the arch is the presence of abundant top-southwest shear-sense indicators on the south side of the arch and top-northeast indicators on the northeast side of the arch. These oppositely directed indicators have been explained previously as cross-cutting shear zones (Naruk and Bykerk-Kaufmann, 1990) and as characteristic features of core complexes that formed in association with uplift and arching during isostatic uplift in response to tectonic denudation (Reynolds and Lister, 1990; see also Wernicke, 1992).

Hundreds of measurements of mylonitic lineation and foliation, collected by the author in preparation of this field guide, are plotted in figure 16. Those measurements of lineation in which shear-sense was apparent in the same outcrop are color coded, green for top northeast shearing and red for top southwest shearing. It is clear from the two plots that shearing was top southwest on the south side of the arch and top northeast on the north side, as previously identified by the two studies cited above. I did not identify any cross-cutting relationships between the two oppositely directed fabrics, in contrast to the study by Naruk and Bykerk-Kaufmann (1990). The fabric on the south side of the arch is more strongly developed, includes ultramylonitic quartz veins (as seen at stop 1), and contains no top-northeast shear-sense indicators. This contrasts with the dominantly top-northeast mylonitic fabric on the north side of the arch, which contains some top-southwest indicators, is not a particularly strong fabric, and generally lacks ultramylonites. From this contrast it appears that the top-southwest fabric on the south side of the arch, which is approximately concordant to the structurally overlying Catalina detachment fault, formed during a time interval that outlasted mylonitization on the north side of the arch. This is suggested because the top-southwest fabric includes highly localized ultramylonitic quartz veins as seen as field stop A2 that are inferred to have formed under the lowest temperature conditions, and because the top-southwest fabric apparently transposed all earlier formed top-northeast fabrics so that none have survived on the south side of the arch.

A striking and perhaps unique feature identified in this study is the change in the trend of mylonitic lineations on the north side of the arch. As is apparent in figure 16 (upper), trend changes from about 065° at the crest of the arch to 040° to 030° at 2.5-3.5 km north of the arch crest. The north-dipping zone strikes eastward east of Molino Canyon, whereas the south dipping zone appears to strike southeastward toward Agua Caliente Hill. Measurements by Ann Bykerk-Kauffman and her students at California State University, Chico, indicate that lineation trend is even more northerly in the north-dipping mylonite zone in these eastern exposures, reaching due north several kilometers east of Molino Canyon. I interpret this relationship as indicating that the north-dipping zone was originally a top-north shear zone that was transposed into parallelism with the south-dipping zone, and that lineations were rotated into parallelism with the top-southwest zone near the crest of the arch, with progressively greater transposition closer to the arch crest.

The Catalina detachment fault is estimated to have approximately 30 km of displacement. To the southeast, on the east side of the Rincon Mountains, a suite of Proterozoic granites intrudes Pinal Schist in the footwall of the detachment fault (Drewes, 1974). This contact, with intruding granites on the east side of the contact, has been displaced to the southwest in the hanging wall of the detachment fault so that the intrusive contact is inferred to be buried beneath the Tucson basin, which requires at least 28.5 km of displacement (Dickinson, 1991). At the west edge of the Santa Catalina Mountains the Granite of Alamo Canyon, a moderately dark, late Cretaceous biotite-hornblende granite or granodiorite (Spencer and Pearthree, 2004), is possibly the footwall equivalent of the mafic border phase of the Amole Granite in the northern Tucson Mountains (Lipman, 1993) which is now about 30 km to the southwest. Displacements of similar or greater magnitude have been inferred for

equivalents of the detachment fault north west of the Santa Catalina Mountains (Richard et al., 2003a).

Restoration of 30 km of displacement on the Catalina detachment fault places the crest of the forerange arch beneath the western Tucson basin and the southeastern Tucson Mountains (Fig. 17). In this location the north-dipping mylonitic shear zone on the north side of the forerange arch projects up dip toward the San Xavier detachment fault in the northeastern Sierrita Mountains. The San Xavier detachment fault is estimated to have at least 16 km of top-north displacement, based on inferred displacement of the San Xavier North porphyry copper ore body from on top of the Pima-Mission ore body and displacement of the Pima-Mission ore body from on top or next to the Twin Buttes ore body (Cooper, 1973; Titley, 1982; Richard et al., 2003b). The San Xavier detachment fault is also possibly correlative with the Coyote Mountain detachment fault to the west, which is underlain by the Coyote Mountain mylonite zone with north-south trending mylonitic lineations and top-north shear-sense (Davis et al., 1987).

My interpretation of the top-northeast mylonite zone on the north side of the forerange arch is that it formed as a top-north shear zone down-dip from the San Xavier detachment fault, and that its originally north-trending lineations have been transposed into more northeasterly trends by top-southwest shearing downdip from the Catalina detachment fault. Both detachment faults displace and were active at the time that Turkey Track porphyry was erupted at about 26-28 Ma (Percious, 1968; Richard et al., 2003b; Spencer et al., 2001). Displacement on the San Xavier fault and its down-dip, top-north mylonitic shear zone apparently ended well before motion ceased on the Catalina detachment fault and its down-dip continuation as a top-southwest mylonitic shear zone, perhaps because it was cut off at depth by the shear zone down dip from the Catalina detachment fault.

References Cited

Anderson, J.L., 1989, Proterozoic anorogenic granites of the southwestern United States, *in* Jenny, J.P., and Reynolds, S.J., eds., Geologic Evolution of Arizona: Arizona Geological Society Digest 17, p. 211-238.

Bykerk-Kauffman, Ann, 1986, Multiple episodes of ductile deformation within the lower plate of the Santa Catalina metamorphic core complex, southeastern Arizona, *in* Beatty, Barbara, and Wilkinson, P.A.K., eds., Frontiers in geology and ore deposits of Arizona and the Southwest: Tucson, Arizona Geological Society Digest, v. 16, p. 460-463.

Cooper, J.R., 1973, Geologic map of the Twin Buttes Quadrangle, southwest of Tucson, Pima County, Arizona: U.S. Geological Survey Miscellaneous Geologic Investigations Map I-745, scale 1:48,000.

Davis, G.H., Gardulski, A.F., and Lister, G.S., 1987, Shear zone origin of quartzite mylonite and mylonitic pegmatite in the Coyote Mountains metamorphic core complex, Arizona: Journal of Structural Geology, v. 9, n. 3, p. 289-297.

Dickinson, W.R., 1991, Tectonic setting of faulted Tertiary strata associated with the Catalina core complex in southern Arizona: Geological Society of America, Special Paper 264, 106 p.

Drewes, H., 1974, Geologic map and sections of the Happy Valley Quadrangle, Cochise County, Arizona: U.S. Geological Survey Miscellaneous Investigations Series Map I-832, scale 1:48,000.

Force, E.R., 1997, Geology and mineral resources of the Santa Catalina Mountains, southeastern Arizona: Tucson, Arizona, Center for Mineral Resources, Monographs in Mineral Resource Science, n. 1, 134 p.

Lipman, P.W., 1993, Geologic map of the Tucson Mountains caldera, southern Arizona: U.S. Geological Survey Miscellaneous Investigations Series Map I-2205, 2 sheets, scale 1:24,000.

Naruk, S.J., and Bykerk-Kauffman, A., 1990, Late Cretaceous and Tertiary deformation of the Santa Catalina metamorphic core complex, Arizona, *in* Gehrels, G.E., and Spencer, J.E., eds., Geologic excursions through the Sonoran Desert region, Arizona and Sonora: Arizona Geological Survey Special Paper 7, p. 41-50.

Percious, J.K., 1968, Geology and geochronology of the Del Bac Hills, Pima County, Ariozna, *in* Titley, S.R., ed., Southern Arizona Guidebook III: Arizona Geological Society, p. 199-207.

Reynolds, S.J., and Lister, G.S., 1990, Folding of mylonitic zones in Cordilleran metamorphic core complexes: Evidence from near the mylonitic front: Geology, v. 18, no. 3, p. 216-219.

Richard, S.M., Spencer, J.E., Ferguson, C.A., Dickinson, W.R., and Orr, T.R., 2003a, Evidence for 35-50 km displacement on the Cloudburst-Suizo detachment fault system north of Tucson, Arizona, and restoration of a Mesozoic high-angle fault system: Geological Society of America Abstracts with Programs, v. 35, n. 6. p. 27.

Richard, S.M., Spencer, J.E., Youberg, A., and Johnson, B.J., 2003b, Geologic map of the Twin Buttes 7 ½' Quadrangle, Pima County, Arizona: Arizona Geological Survey Digital Geologic Map DGM-31, scale 1:24,000.

Spencer, J.E., and Pearthree, P.A., 2004, Geologic map of the Oro Valley 7 ½' Quadrangle, Pima County, Arizona: Arizona Geological Survey Digital Geologic Map 21, version 2.0, scale 1:24,000.

Spencer, J.E., Ferguson, C.A., Richard, S.M., Orr, T.R., Pearthree, P.A., Gilbert, W.G., and Krantz, R.W., 2001, Geologic map of The Narrows 7 ½' Quadrangle and the southern part of the Rincon Peak 7 ½' Quadrangle, eastern Pima County, Arizona: Arizona Geological Survey Digital Geologic Map 10, layout scale 1:24,000, with 32 p. text (revised May, 2002).

Titley, S.R., 1982, Some features of tectonic history and ore genesis in the Pima mining district, *in* Titley, S.R., ed., Advances in geology of the porphyry copper deposits, southwestern North America: Tucson, University of Arizona Press, p. 387-406.

Figure 16 (next page). A. Lineation trend versus distance from the axis of the forerange arch. B. Lineation plunge versus distance from the forerange arch.

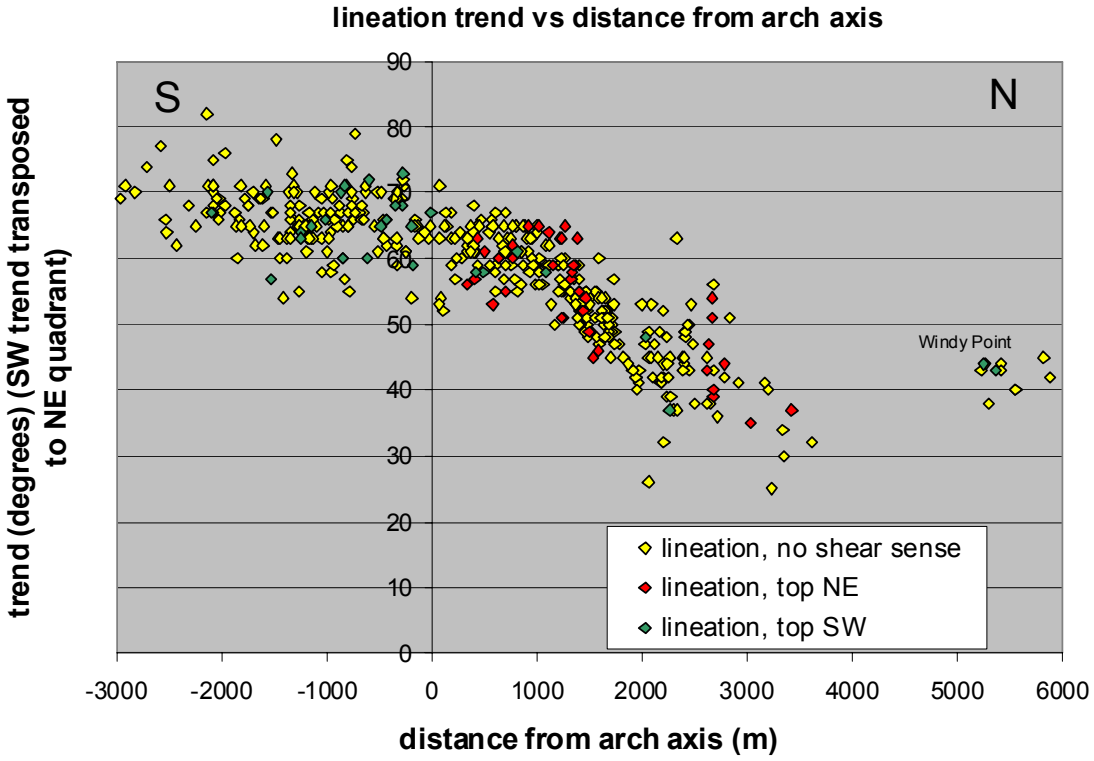
lineation trend vs distance from arch axis
S
N
Windy Point
lineation, no shear sense
lineation, top NE
lineation, top SW
trend (degrees) (SW trend transposed to NE quadrant)
distance from arch axis (m)
90
80
70
60
50
40
30
20
10
0
-3000
-2000
-1000
0
1000
2000
3000
4000
5000
6000

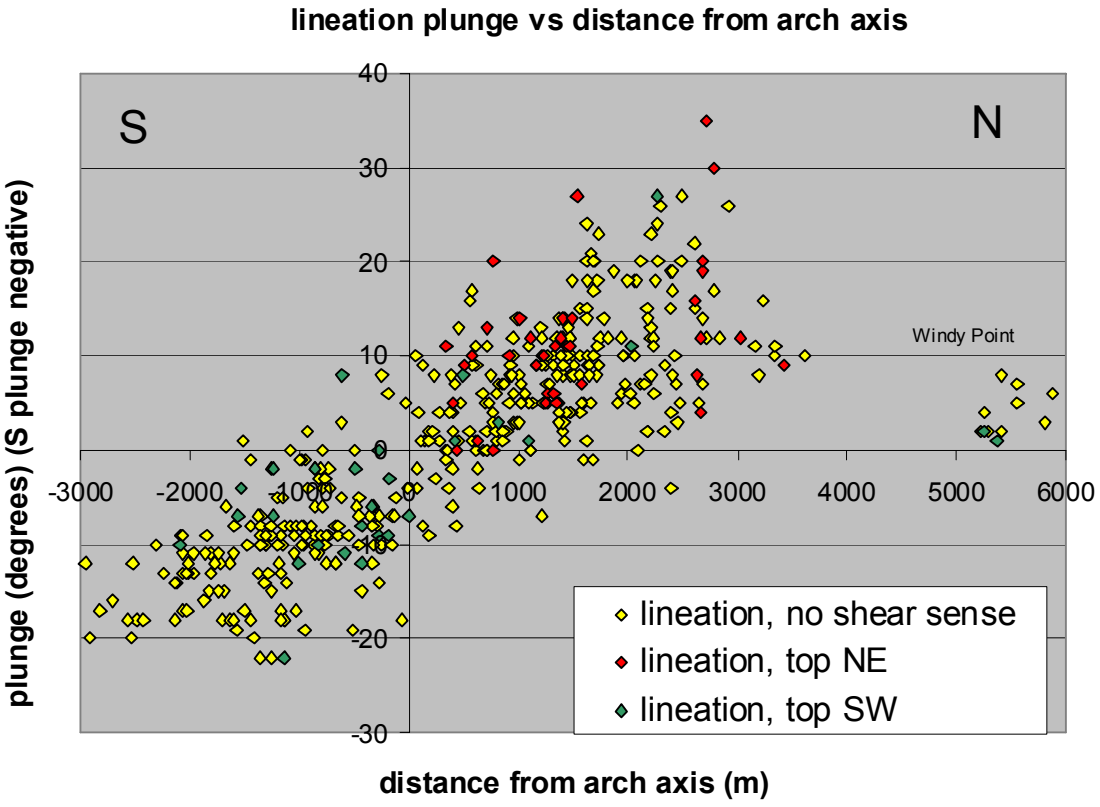
lineation plunge vs distance from arch axis
S
N
Windy Point
lineation, no shear sense
lineation, top NE
lineation, top SW
plunge (degrees) (S plunge negative)
distance from arch axis (m)
40
30
20
10
0
-10
-20
-30
-3000
-2000
-1000
0
1000
2000
3000
4000
5000
6000

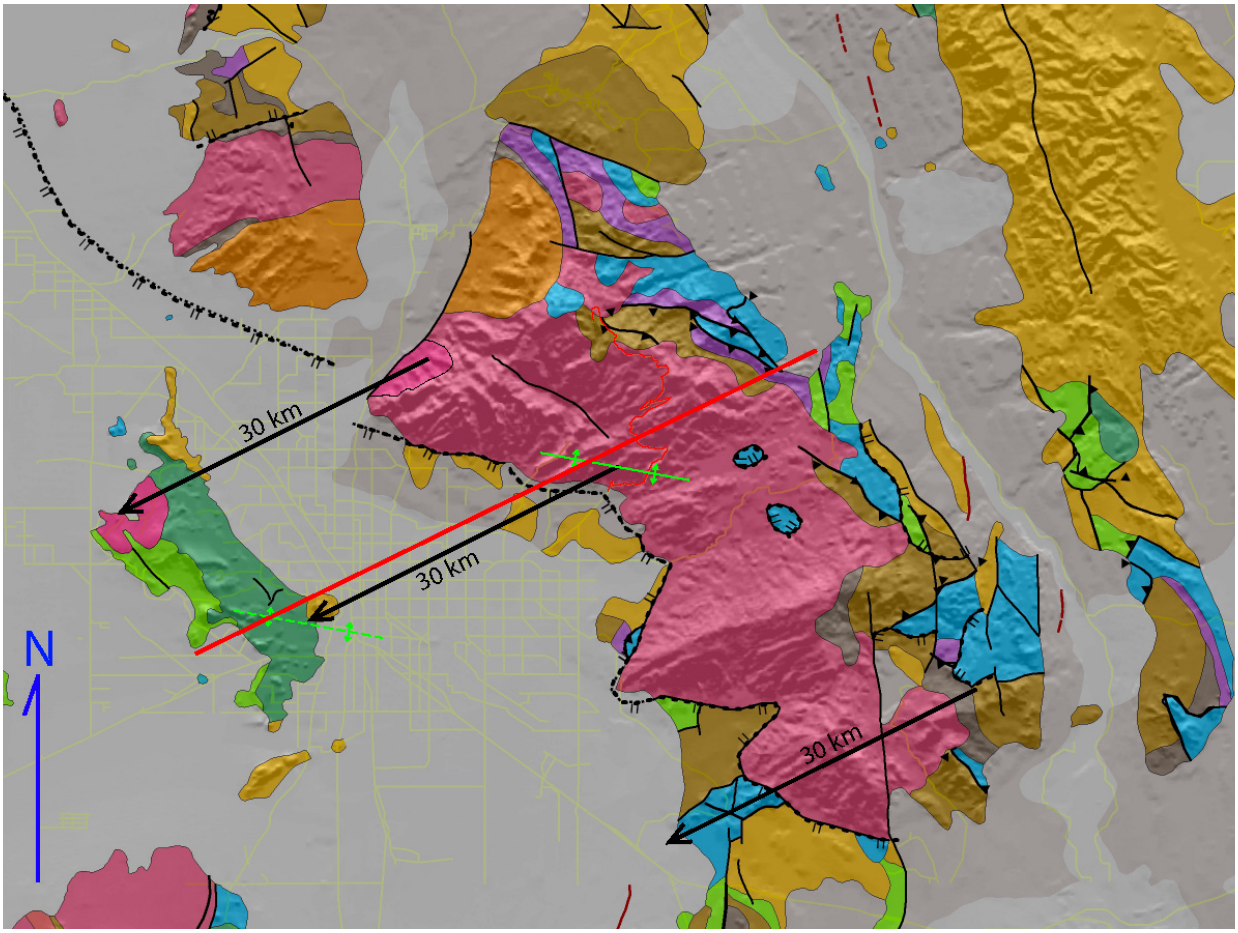

Figure 17 (page after next page). Geologic map of the Santa Catalina Mountains and surrounding areas. Estimated 30 km displacement vectors shown for northwestern and southeastern displaced features. Also shown is 30 km vector to restore the forerange arch to beneath the Tucson Mountains.

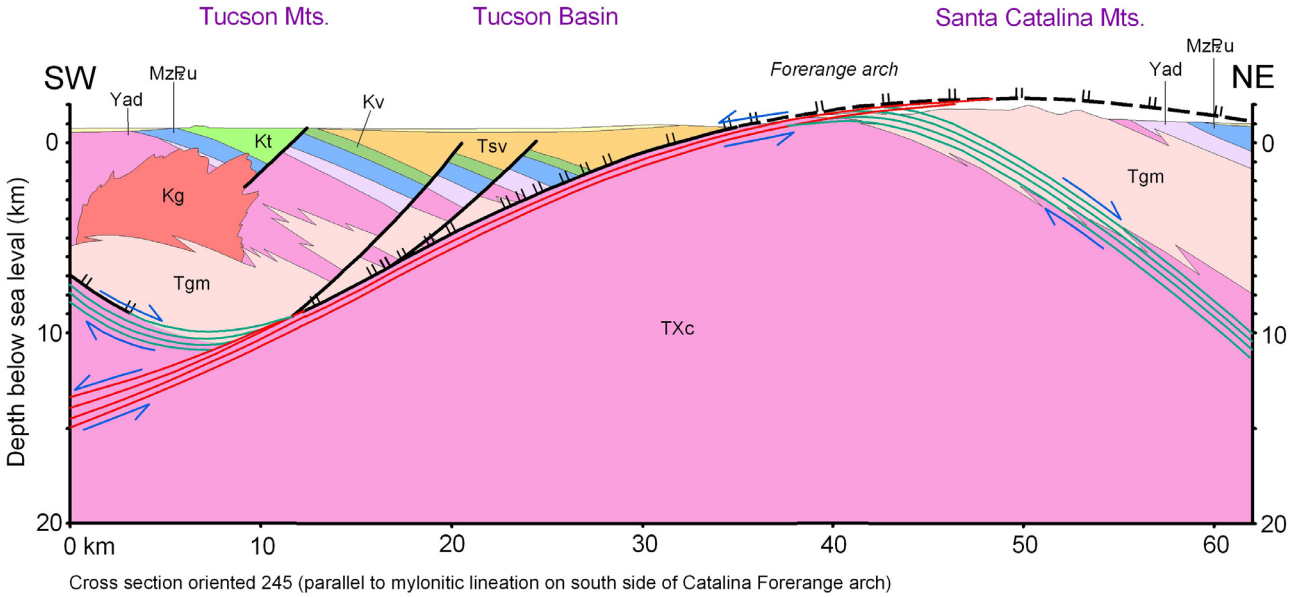

Figure 18. Cross section from Santa Catalina Mountains across the Tucson basin to the Tucson Mountains. Location shown by red line in figure 17. Note displacement and separation of north-dipping mylonite zone.

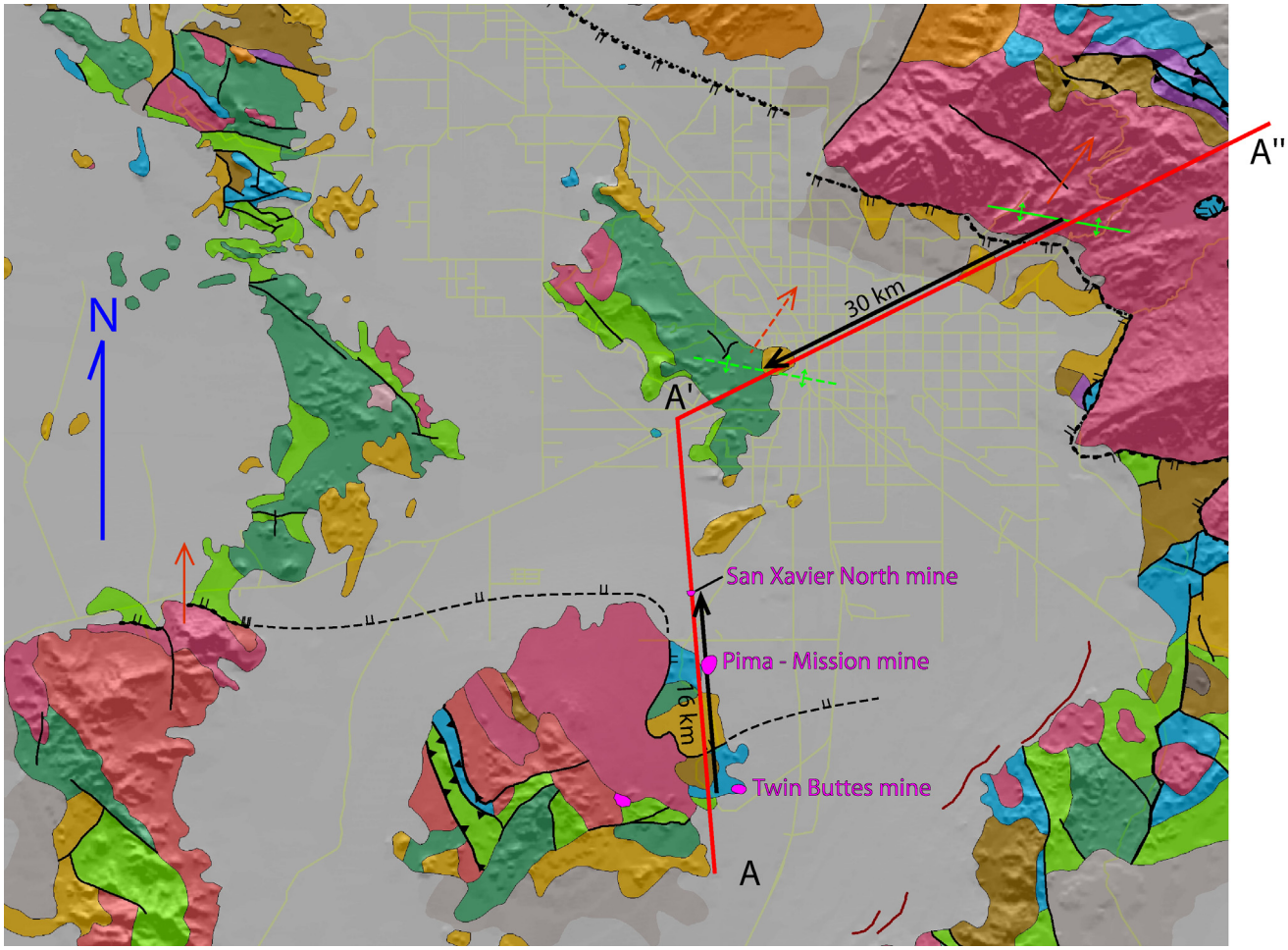

Figure 19. See figure caption on next page.

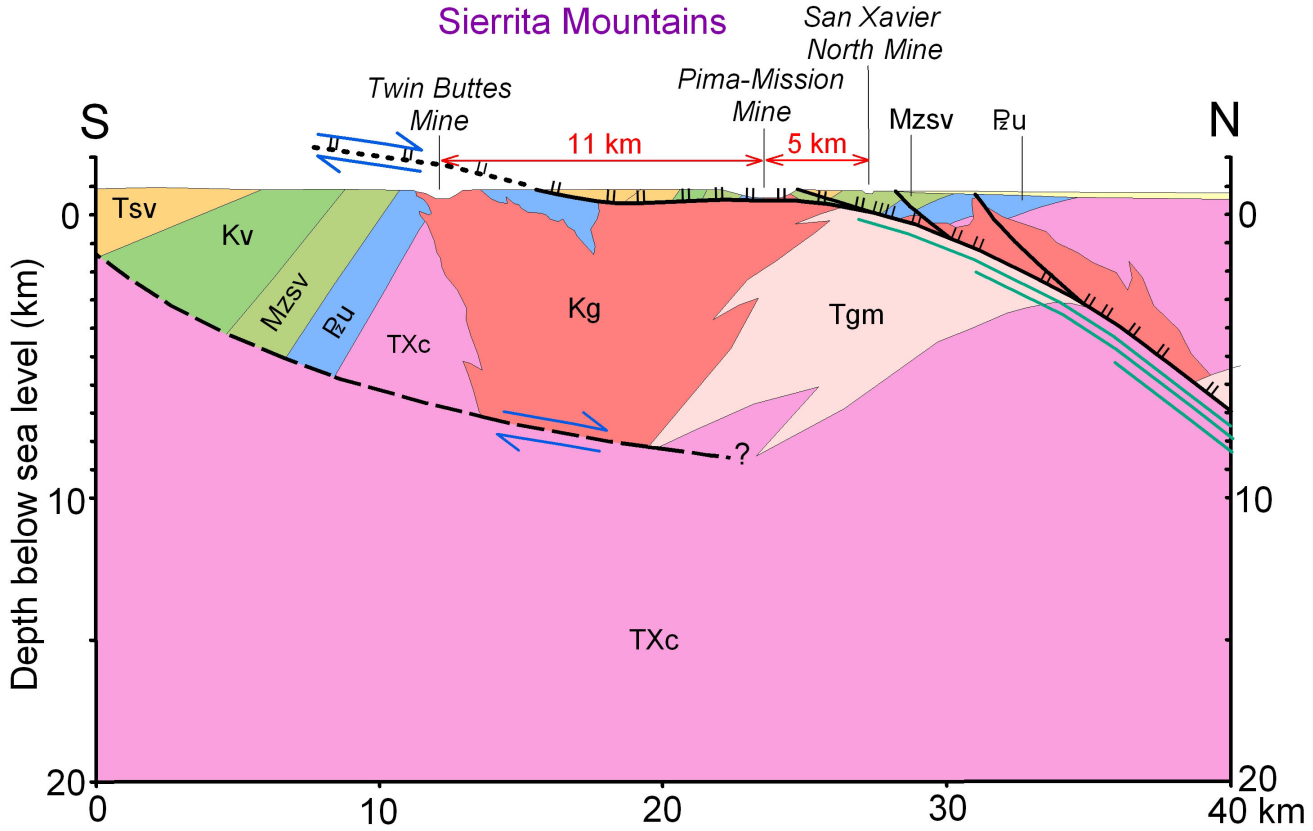

Figure 20. Cross section A-A', location shown on figure 19.

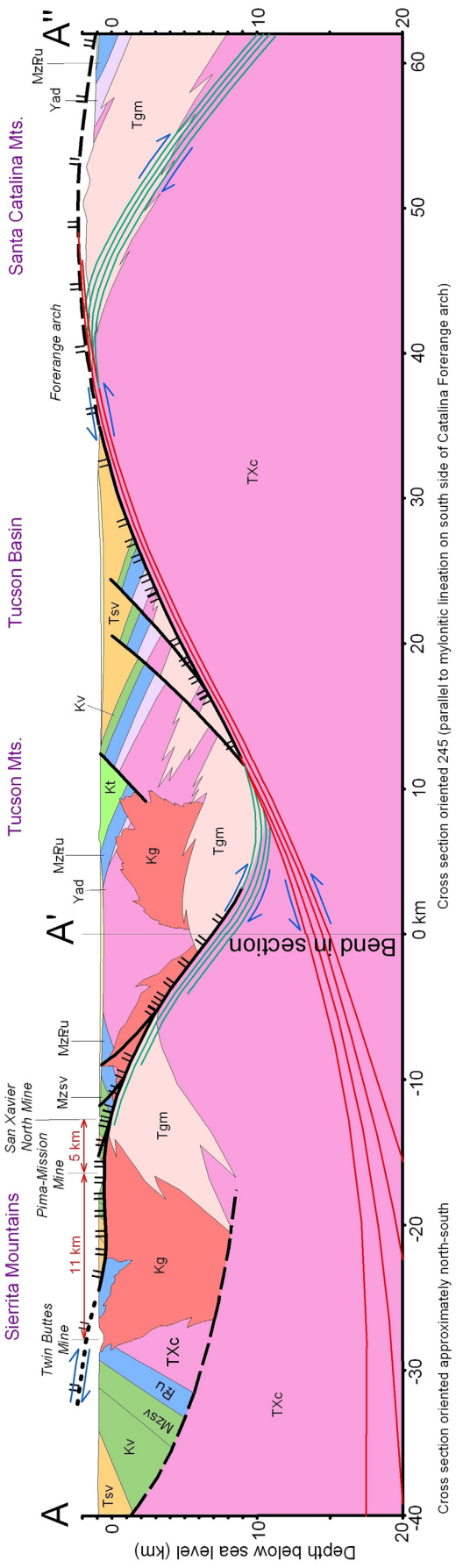

Figure 19 (previous page, top). Geologic map of the greater Tucson area and Avra Valley area to the west. Also shown are locations of four large Cretaceous porphyry copper mines in the Sierrita Mountains. Cross section A-A', shown in figure 20, is drawn parallel to the approximately 16 km displacement vector for dismemberment of the Twin Buttes – Pima–Mission – San Xavier North ore body system. The San Xavier detachment fault in the Sierrita Mountains is correlated with the Coyote Mountain detachment fault to the west, which overlies a mylonitic shear zone with top-north normal-shear indicators represented by the red arrow.

Figure 21. Combined cross section A-A' (Figure 20) and A'-A" (Figure 18). Location shown in figure 19. Note approximately 70° bend in section at A'.

FIELD GUIDE TO THE WINDY POINT SHEAR ZONE

Highway Stops #4 and #5: Windy Point and Geology Vista. Stop at the Windy Point parking area (restrooms here) or, a little further up the highway, the Geology Vista parking area (Fig. 22). From the Windy Point parking area, walk (there is no official trail here, the "walk" is more of a scramble up a rocky slope) up a small gully behind the eastern part of the parking lot that is on the inside corner of the hairpin turn. Or, from the Geology Vista parking lot, walk southwest along the left side of the highway until you reach the base of a small hill that is the high point between the two parking lots, and then walk to the hill top by way of the left (southeast) side of the hill (leave the highway where the guard rail ends). The mylonitic deformation in these rocks is best developed at the ridge crest, and dies out downward over 20-40 m of structural thickness (Windy Point zone of Force, 1997). Lineation plunges 1° to 8° to the northeast. Foliation is subhorizontal but difficult to accurately measure. I identified several top-southwest shear-sense indicators at two locations in this mylonite zone (Fig. 22; Table 4), but all are somewhat equivocal.

At stop D1, a vertical slab protrudes from the ridge crest about 70 m southwest of the highest point on the ridge (Fig. 23). Top-southwest shear-sense indicators on both the northwest and southeast sides of this rock illustrate some of the difficulties of shear-sense interpretation. On the southwest side of the rock, a quartz veinlet is in contact with a large K-feldspar phenocryst on the bottom and left (southwest) side of the crystal, but where it reaches the top of the phenocryst extends away from it for perhaps 10 cm (Fig. 24). This 10 cm quartz veinlet is possibly sheared away from the top of the K-feldspar phenocryst along a subhorizontal shear zone that directly overlies the phenocryst. If this interpretation is correct it indicates top-southwest shearing. Below the K-feldspar phenocryst, and above the left end of the sheared quartz veinlet, foliations are locally tilted to the right but are truncated by the through-going, subhorizontal shear zones (Fig. 24). Truncation of the inclined foliation by the through-going subhorizontal foliation is a typical relationship between S (flattening) and C (shearing) surfaces in an S-C mylonite that here indicates top-southwest shearing.

C' surfaces are C surfaces in an S-C mylonite that dip forward in a broader shear zone (i.e., are inclined toward the displacement direction of structurally higher rocks). Near the feature described above is a possible C' surface that cuts across a pegmatitic layer in the layered leucogranite and dips gently to the left (southwest; Fig. 25). Within this pegmatitic layer are somewhat irregular layers that dip to the northeast, obliquely to the subhorizontal boundaries of the pegmatitic granite layer, and are truncated by the planar C' surface. I interpret these as S surfaces that are truncated by a C' surface in a manner that indicates top-southwest shearing. Another C' surface visible on the northwest side of this rock indicates top-southwest shearing (Fig. 26), as do C' surfaces at stop D2.

Table 4: Windy Point - Geology Vista field stops

Stop No.	UTME*	UTMN*	Feature	Station
D1	526922	3581215	top-southwest shear-sense indicators	JES-05-670
D2	526810	3581112	top-southwest shear-sense indicator	JES-05-673

**NAD 27, zone 12*

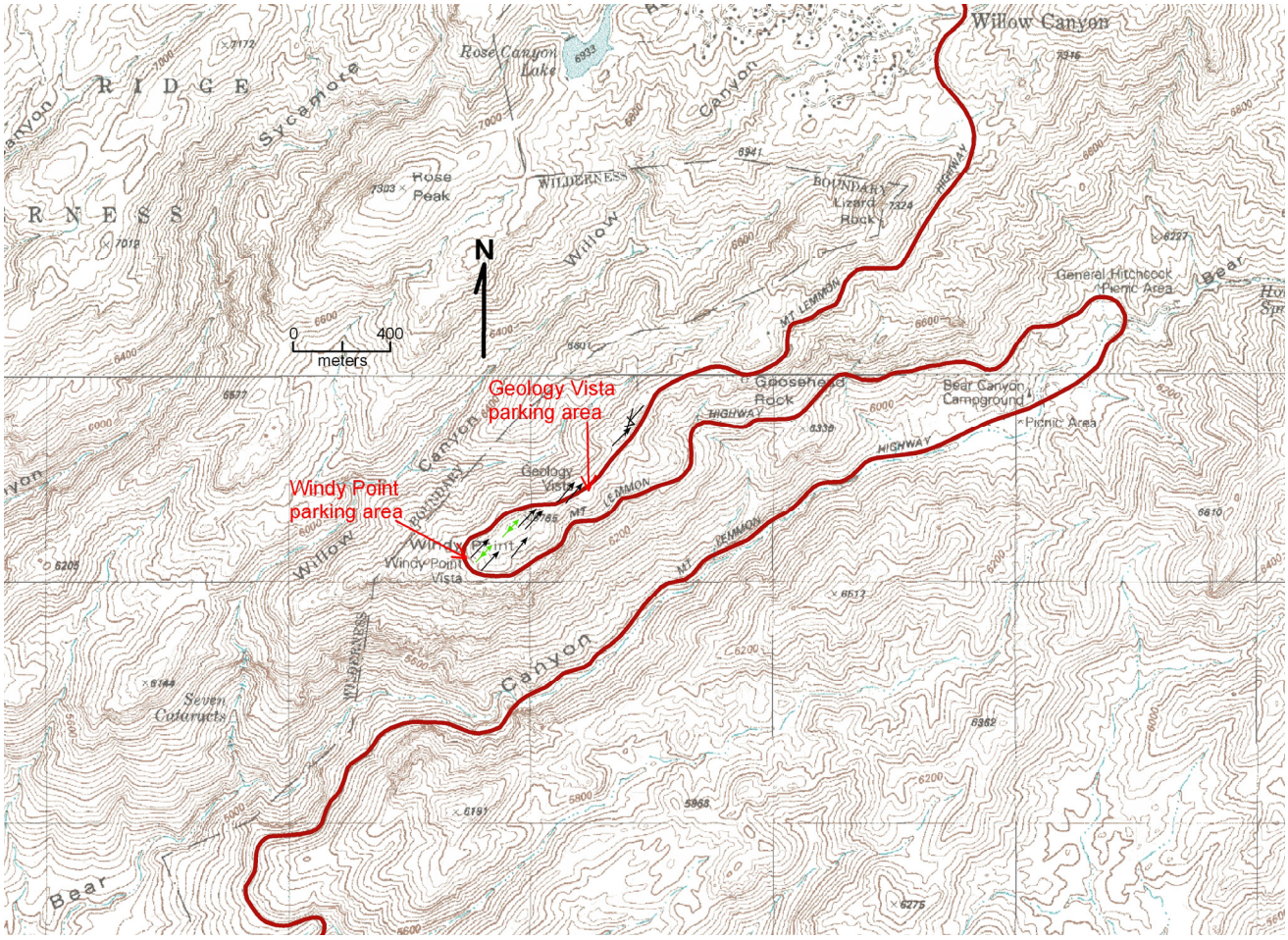

Fig. 22 (above and below). Map figures of Windy Point and Geology Vista areas. Top-southwest indicators in green.

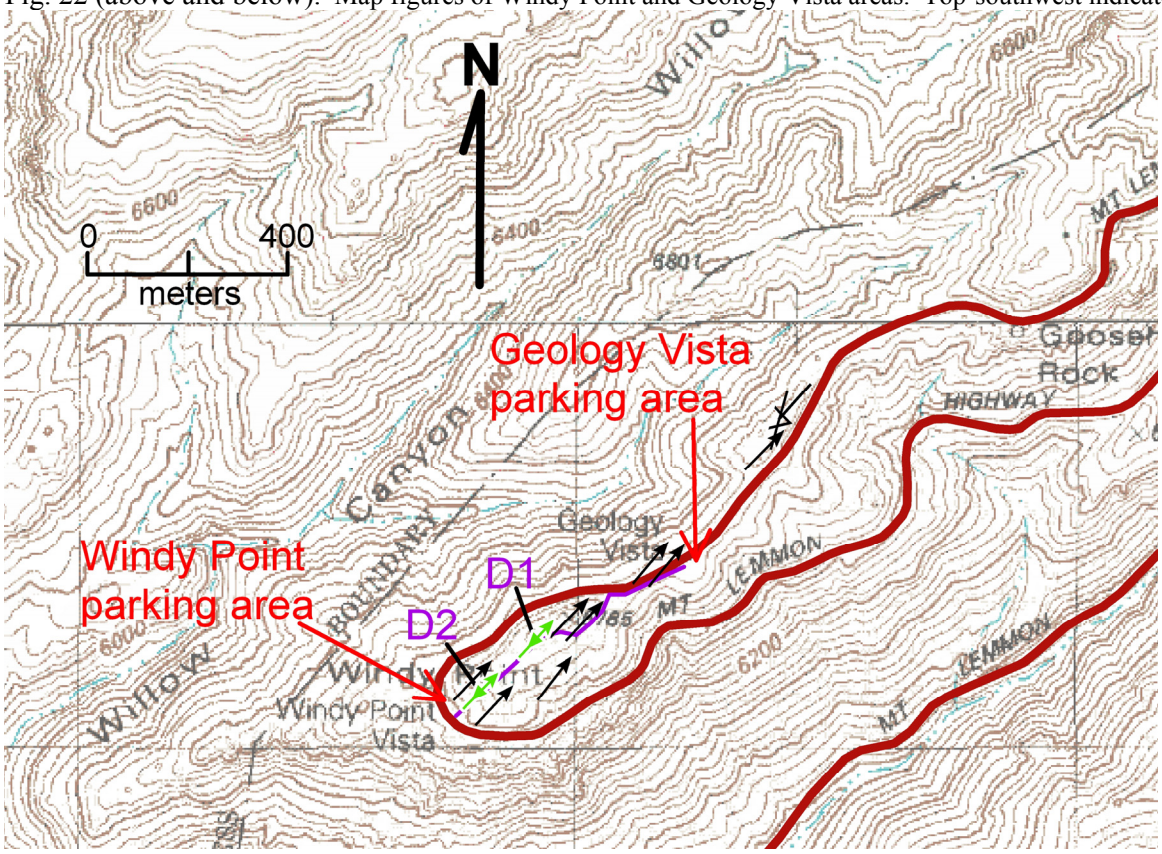

Figure 23. Outcrop field-stop D1, looking southwest after 2003 Aspen fire.

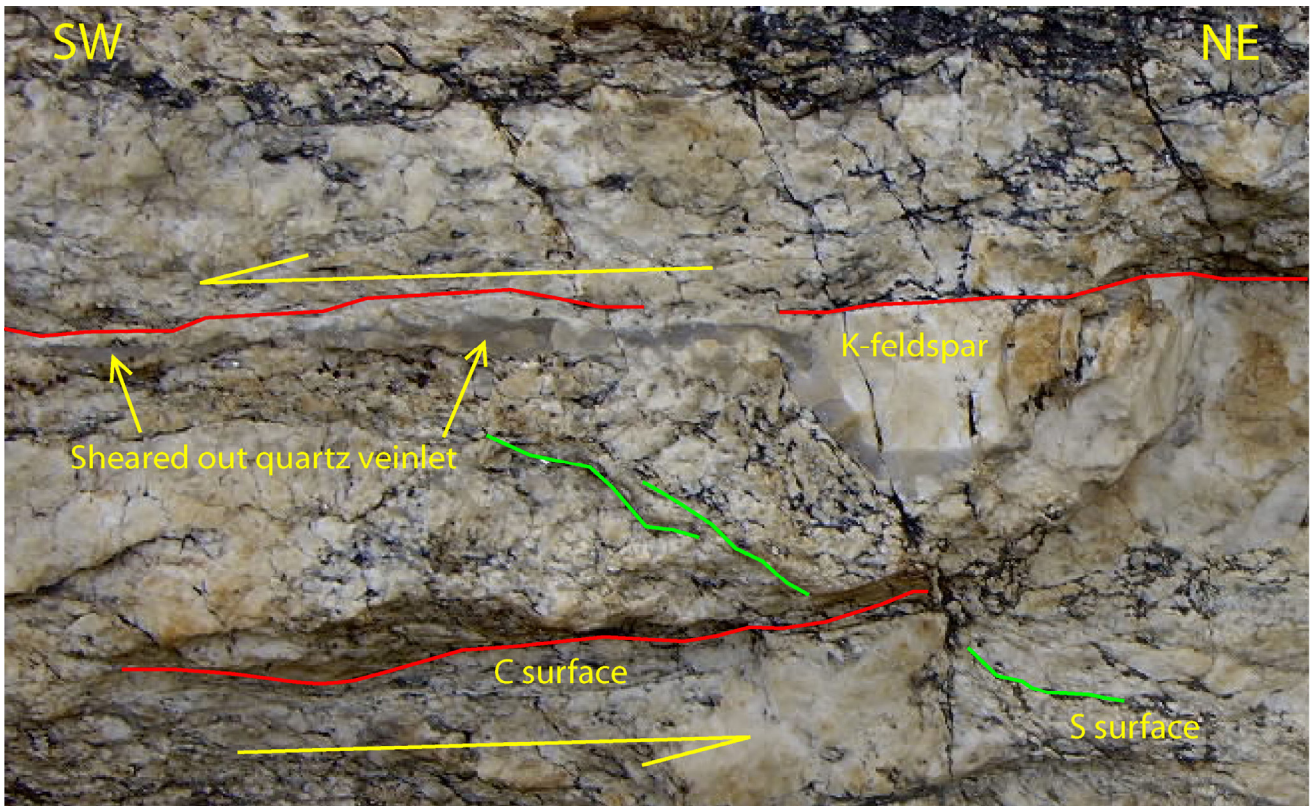

Figure 24. S-C shear-sense indicator and sheared-out quartz veinlet on southeast side of rock at field stop D1. Indicators are somewhat equivocal.

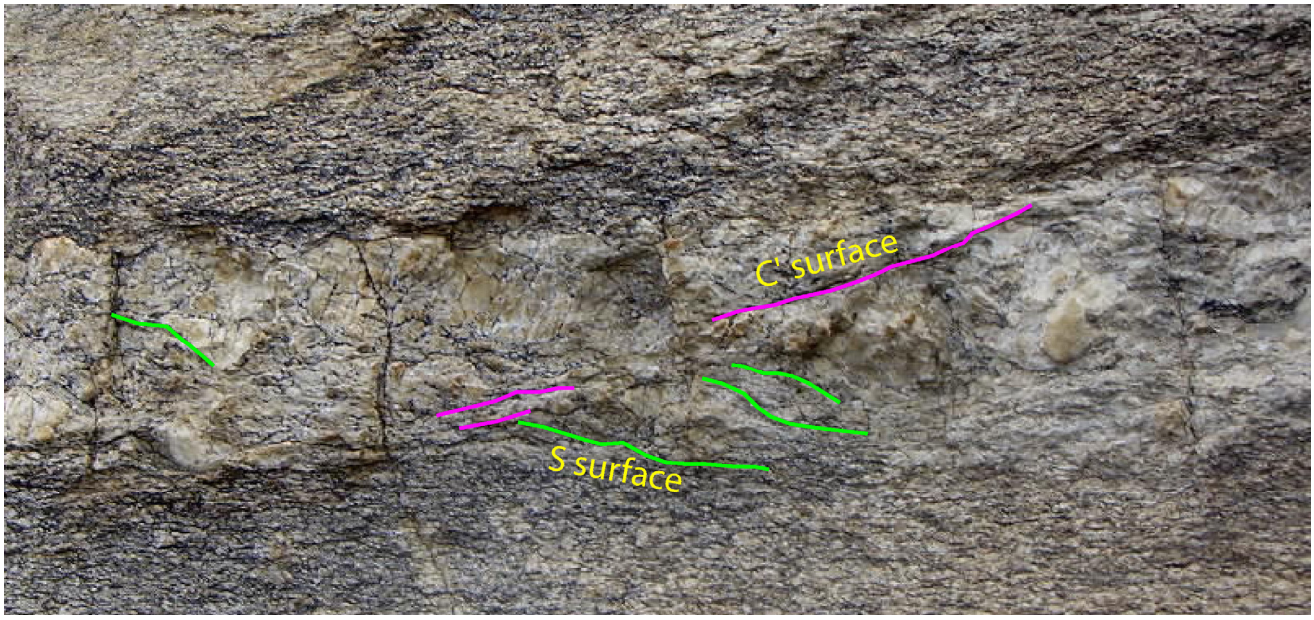

Figure 25. C' surface cutting S surfaces in weak S-C mylonite suggesting top-southwest (left) shearing. Southeast side of rock at field stop D1.

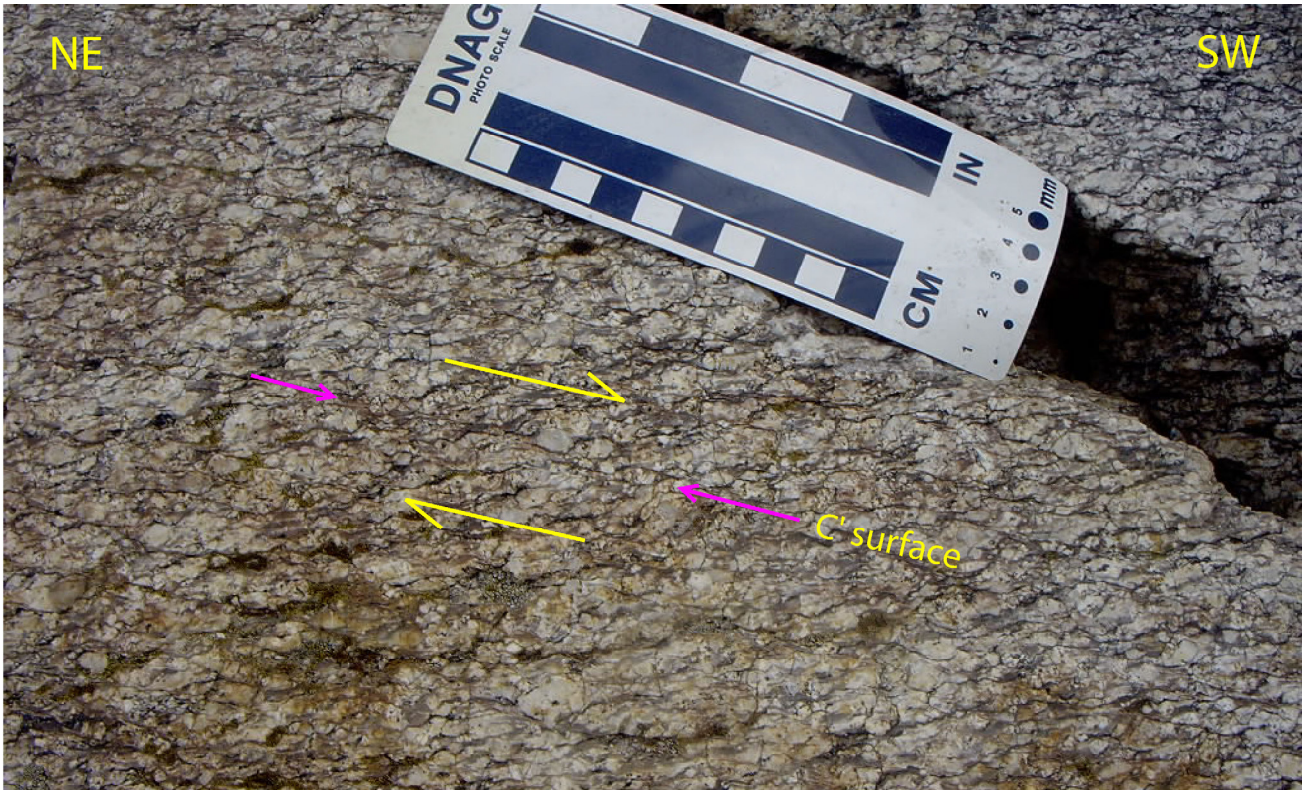

Figure 26. C' surface cutting S surfaces in weak S-C mylonite suggesting top-southwest (right) shearing. Northwest side of rock at field stop D1.

Bear Canyon from Geology Vista and the origin of linear, extension-parallel drainages

Geology Vista provides an excellent view into upper Bear Canyon, which has a remarkably linear course (~241°) over 10 km before it bends southward within the Catalina Forerange to follow the trace of a high-angle fault (Fig. 27; Force, 1997). This straight segment is oriented parallel to the mylonitic lineations on the south side of the Catalina Forerange (240°-250°), and is highly oblique (by 50°-60°) to the regionally southward slope of the south side of the Santa Catalina Mountains.

Lineation-parallel drainages are common in Arizona's metamorphic core complexes (Pain, 1985; Spencer, 2000). They were first identified by Australian geomorphologist Colin Pain, who proposed that the drainages were initially incised into the footwalls of detachment faults as the footwalls were tectonically uncovered, and that within a core complex the youthful drainages flowed down slope on an inclined, freshly exhumed fault plane. Then, once the drainages were incised, the footwalls were folded about lineation-parallel fold axes so that drainages no longer flowed down the steepest course but rather somewhat sideways on the flanks of gently plunging antiformal arches, or along the arch crests (Pain, 1985).

This interpretation requires that the crystalline rocks that make up metamorphic core complexes were folded into some very large folds. Tanque Verde Ridge, which makes up most of the visible Rincon Mountains as seen from Geology Vista (the very large and long ridge ~15-20 km to the southeast), would be a large antiformal fold if this theory is correct. However, there is no indication that rocks structurally above the Catalina detachment fault are also folded, as they should be if folding occurred after detachment faulting. Much detailed mapping in all of Arizona's metamorphic core complexes has failed to identify any structures that could be interpreted as indicating that detachment-fault corrugations are folds produced during a tectonic regime of horizontal compression perpendicular to fold axes. In contrast, post-detachment reverse faults in crystalline rocks and folds in sedimentary rocks have been identified with trends at high angles to corrugations, not parallel to them (e.g., Spencer and Reynolds, 1989; Spencer et al., 2001; Orr et al., 2004). It thus seems more likely that the corrugations of detachment-fault footwalls are giant fault grooves rather than folds produced after footwall exhumation (Spencer, 1999).

Another possibility is that linear drainages were incised during exhumation because canyons in the hanging-wall block maintained hydraulic connection with their lengthening upstream reaches in the footwall block and so guided the drainages down the freshly exhumed fault footwall as it was uncovered (Fig. 28; Spencer, 2000). This would occur only if there is a canyon in the hanging-wall block. Exposures of hanging-wall rocks at the south foot of the Santa Catalina Mountains in the Catalina Foothills consist of mid-Tertiary clastic rocks (primarily fanglomerates), some of which contain mylonitic debris. It thus seems more likely that these sediments were deposited in alluvial fans at the foot of the range, not transported through hanging-wall canyons.

An alternative is that small grooves in the fault footwall, when freshly uncovered by normal faulting, localized drainages into linear forms. The foot of the Santa Catalina Mountains has a significant offset at the mouth of Sabino Canyon, which could represent a synformal groove in the concealed detachment fault. Projected up plunge parallel to mylonitic lineation, this offset is aligned with upper Bear Canyon, and thus is consistent with a causative relationship between a km-scale fault groove and a linear drainage. This offset is, however, at least partly the consequence of offset by a post-detachment high-angle fault that is visible within Sabino Canyon (Force, 1997).

In contrast, two conspicuous linear drainages in the Rincon Mountains, one slightly south of the crest of Tanque Verde Ridge and the other on the crest of Posta Quemada Ridge, are located on the crests of footwall grooves, not in intergroove troughs (Spencer, 2000). It is possible that small, 10-100 m scale grooves that have not been discerned in the trace of the detachment fault at the foot of the Rincon Mountains are responsible for the linear form of these drainages, but if the grooves were small, then it is difficult to account for the km-scale width of the drainage catchments.

In conclusion, two mechanisms appear to be viable possibilities for inception of lineation-parallel drainages. Localization by synformal fault grooves seems more likely for Bear Canyon because it has a possible groove in the right place, and because hanging-wall conglomerates were most likely deposited in alluvial fans emanating from the base of the ancestral Santa Catalina Mountains, which is not an environment likely to provide a canyon that guided stream incision for 10 km down the footwall as it was uncovered. In contrast, in the Rincon Mountains it seems more likely that hanging-wall canyons guided drainage development, and at least one hanging-wall canyon is still preserved (Spencer, 2000). In either case, as you look into upper Bear Canyon with its remarkably linear trend, consider that initial incision occurred as the Santa Catalina Mountains were displaced up and out from beneath the Tucson Basin about 20 m.y. ago, and that somehow, the linear drainage developed parallel to fault displacement direction as inferred from the orientation of megagrooves such as Tanque Verde Ridge and from mylonitic lineations on the south flank of the Santa Catalina Mountains.

References cited

Force, E.R., 1997, Geology and mineral resources of the Santa Catalina Mountains, southeastern Arizona: Tucson, Arizona, Center for Mineral Resources, Monographs in Mineral Resource Science, n. 1, 134 p.

Orr, T.R., Shipman, T.C., and Spencer, J.E., 2004, Geologic map of the North of Oracle 7 ½' Quadrangle, southeastern Pinal County, Arizona: Arizona Geological Survey Digital Geologic Map 23, v. 2.0, scale 1:24,000.

Pain, C.F., 1985, Cordilleran metamorphic core complexes in Arizona: A contribution from geomorphology: Geology, v. 13, p. 871-874.

Spencer, J.E., 1999, Geologic continuous casting below continental and deep-sea detachment faults and at the striated extrusion of Sacsayhuamán, Peru: Geology, v. 27, p. 327-330.

Spencer, J.E., 2000, Possible origin and significance of extension-parallel drainages in Arizona's metamorphic core complexes: Geological Society of America Bulletin, v. 112, p. 727-735.

Spencer, J.E., and Reynolds, S.J., 1989, Tertiary structure, stratigraphy, and tectonics of the Buckskin Mountains, *in* Spencer, J.E., and Reynolds, S.J., Geology and mineral resources of the Buckskin and Rawhide Mountains, west-central Arizona: Arizona Geological Survey Bulletin 198, p. 103-167.

Spencer, J.E., Ferguson, C.A., Richard, S.M., Orr, T.R., Pearthree, P.A., Gilbert, W.G., and Krantz, R.W., 2001, Geologic map of The Narrows 7 ½' Quadrangle and the southern part of the Rincon Peak 7 ½' Quadrangle, eastern Pima County, Arizona: Arizona Geological Survey Digital Geologic Map 10, layout scale 1:24,000, with 32 p. text (revised May, 2002).

Figure 27 (next page, upper). Shaded relief map of the Santa Catalina Mountains and surrounding areas, showing lineation-parallel canyons. Point A in lower Bear Canyon is location of fault that deflects trend of drainage (Force, 1997).

Figure 28 (next page, lower). Three-step diagram of development of an extension-parallel drainage due to displacement on a low-angle normal fault. Red arrow is displacement vector. (A) Before slip. (B) After one slip event. (C) After three slip events. If angle α is less than 90°, water flowing over freshly denuded footwall will contact fault and then follow fault trace until entering canyon in hanging-wall block. Incision into footwall and progressive displacement will then produce an elongating, extension-parallel drainage (from Spencer, 2000).

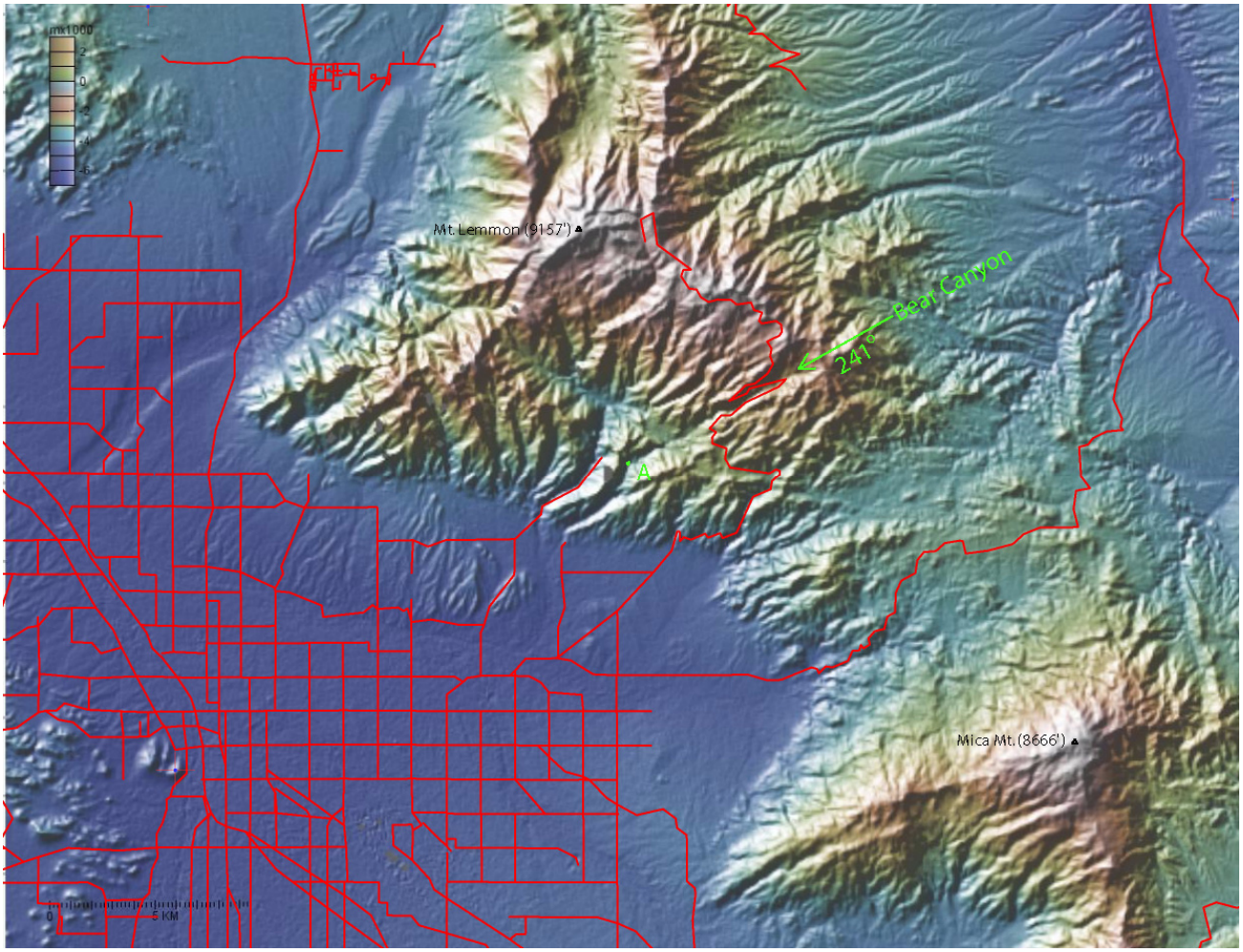

Figure 27.

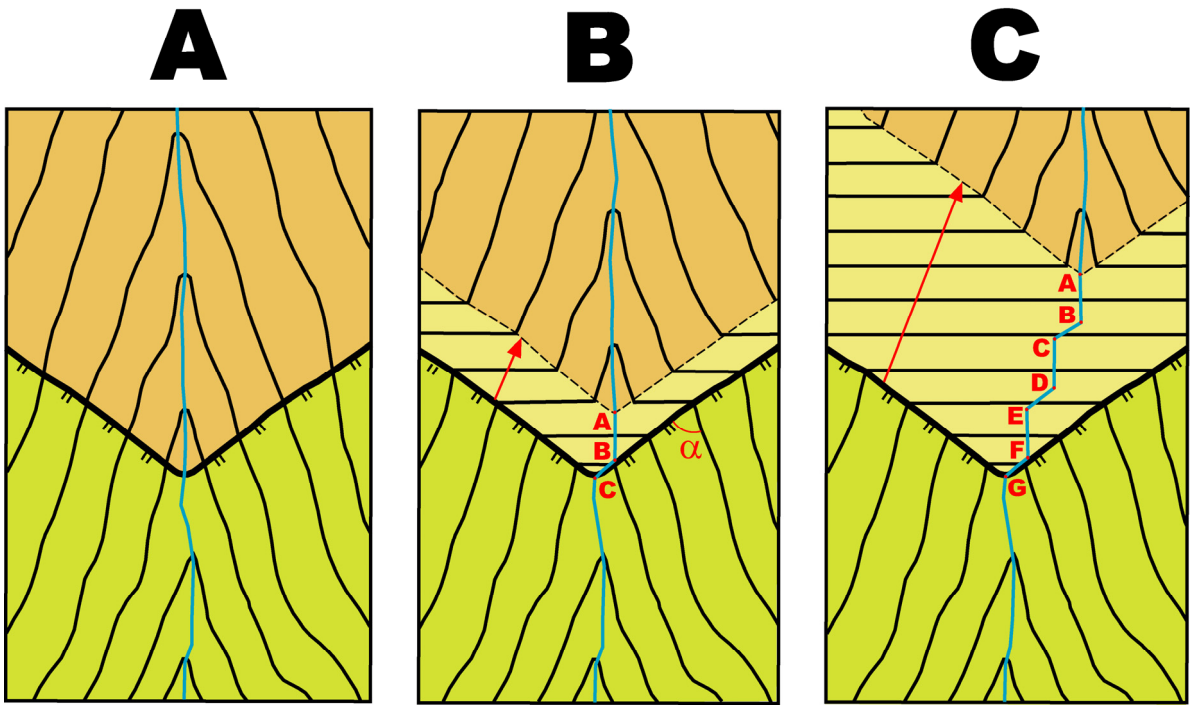

Figure 28.